

Viral alpha-synuclein knockdown prevents spreading synucleinopathy

Sindhu Menon,^{1,*} Rikke H. Kofoed,^{2,*} Fadl Nabouh,¹  Kristiana Xhima,^{2,3} Yasmeen Al-Fahoum,¹ Tammy Langman,¹ Howard T.J. Mount,^{1,4,5} Lamya S. Shihabuddin,^{6,†} S. Pablo Sardi,⁶ Paul E. Fraser,^{1,7} Joel C. Watts,^{1,8} Isabelle Aubert^{2,3} and  Anurag Tandon^{1,9}

* These authors contributed equally to this work.

† Present address: 5AM Ventures, Boston, MA, USA.

The accumulation of aggregated alpha-synuclein (α -syn) in Parkinson's disease, dementia with Lewy bodies and multiple system atrophy is thought to involve a common prion-like mechanism, whereby misfolded α -syn provides a conformational template for further accumulation of pathological α -syn. We tested whether silencing α -syn gene expression could reduce native non-aggregated α -syn substrate and thereby disrupt the propagation of pathological α -syn initiated by seeding with synucleinopathy-affected mouse brain homogenates. Unilateral intracerebral injections of adeno-associated virus serotype-1 encoding microRNA targeting the α -syn gene reduced the extent and severity of both the α -syn pathology and motor deficits. Importantly, a moderate 50% reduction in α -syn was sufficient to prevent the spread of α -syn pathology to distal brain regions. Our study combines behavioural, immunohistochemical and biochemical data that strongly support α -syn knockdown gene therapy for synucleinopathies.

- 1 Tanz Centre for Research in Neurodegenerative Diseases, Toronto, ON M5T 0S8, Canada
- 2 Sunnybrook Research Institute, Toronto, ON M4N 3M5, Canada
- 3 Department of Laboratory Medicine and Pathobiology, University of Toronto, Toronto, ON M5S 1A1, Canada
- 4 Department of Psychiatry, University of Toronto, Toronto, ON M5S 1A1, Canada
- 5 Department of Physiology, University of Toronto, Toronto, ON M5S 1A1, Canada
- 6 Sanofi, Framingham, MA 01701, USA
- 7 Department of Medical Biophysics, University of Toronto, Toronto, ON M5S 1A1, Canada
- 8 Department of Biochemistry, University of Toronto, Toronto, ON M5S 1A1, Canada
- 9 Department of Medicine, University of Toronto, Toronto, ON M5S 1A1, Canada

Correspondence to: Anurag Tandon, PhD

Tanz Centre for Research in Neurodegenerative Diseases, University of Toronto, Krembil Discovery Tower

Rm. 4KD481, 60 Leonard Ave, Toronto, ON M5T 0S8, Canada

E-mail: a.tandon@utoronto.ca

Keywords: Parkinson's disease; multiple system atrophy; gene therapy; gene silencing; pathology

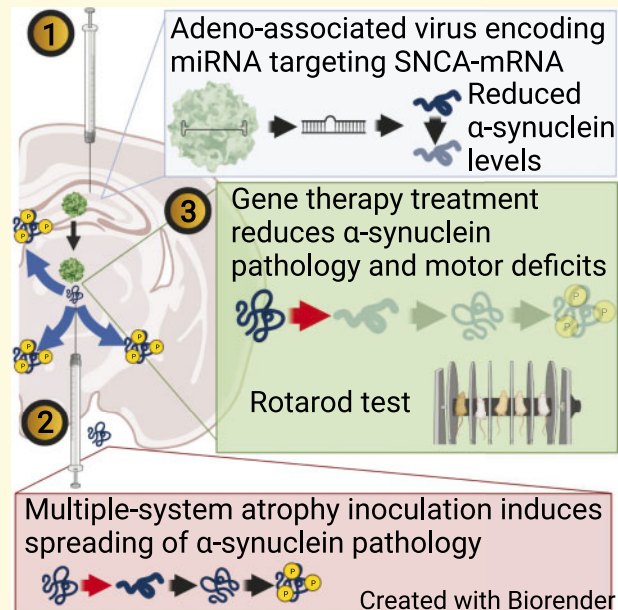
Abbreviations: α -syn = alpha-synuclein; AAV1 = adeno-associated virus serotype-1; AP = anterior–posterior; ASO = antisense oligonucleotide; CBA = chicken β -actin; DAT = dopamine transporter; dpi = days post-inoculation; DV = dorsal–ventral; eGFP = enhanced green fluorescent protein; GFAP = glial fibrillary acidic protein; Iba1 = ionized calcium-binding adapter molecule 1; miR = microRNA; ML = medial-lateral; MSA = multiple system atrophy; MSA_{mo} = MSA inoculum-derived mouse brain homogenate; NeuN = neuronal nuclei; p-syn = phospho-Ser129- α -syn; SN = substantia nigra; TH = tyrosine hydroxylase; VG = vector genome

Received July 14, 2021. Revised July 14, 2021. Accepted July 17, 2021. Advance Access publication October 22, 2021

© The Author(s) (2021). Published by Oxford University Press on behalf of the Guarantors of Brain.

This is an Open Access article distributed under the terms of the Creative Commons Attribution License (<https://creativecommons.org/licenses/by/4.0/>), which permits unrestricted reuse, distribution, and reproduction in any medium, provided the original work is properly cited.

Graphical Abstract



Introduction

Synucleinopathies comprise a clinically diverse group of neurodegenerative disorders with a common pathological trait, an accumulation of phosphorylated, misfolded and detergent-insoluble alpha-synuclein (α -syn). The α -syn is compartmentalized within intracellular inclusions predominantly within neurons in Parkinson's disease and dementia with Lewy bodies, and in glia in multiple system atrophy (MSA).¹ In healthy cells, α -syn structure likely shifts between intrinsically disordered and alpha-helical forms, although various triggers, including mutations, oxidative stress and impaired proteostasis, induce the accumulation of α -syn species with high β -sheet content.²⁻⁴ The misfolded α -syn is more conformationally restricted and can self-amplify by organizing native α -syn into oligomers and fibrils *in vitro*.⁵⁻⁸ This mechanism, proposed to underlie a prion-like spread of α -syn pathology across distal but connected brain regions, has been demonstrated experimentally in animal models following intracerebral seeding either with recombinant pre-formed α -syn fibrils or with human synucleinopathy brain homogenates.⁹⁻¹⁴ For example, a single inoculation with brain homogenates from post-mortem human MSA, but not age-matched healthy controls, induces bilateral accumulation of insoluble, phosphorylated α -syn inclusions in murine brains. The mice develop a severe and progressive clinicopathological syndrome, characterized by profound motor deficits including progressive ataxia, hind limb paresis and weight loss, reaching clinical disease endpoint within 90–150 days. The resulting synucleinopathy from inoculated mice can be serially propagated in healthy mice that express human α -syn.^{11,12,15}

The susceptibility of neurons to template-induced pathology is proportional to their endogenous α -syn expression.¹⁶ Therefore, to test whether α -syn knockdown offers a treatment strategy to reduce the spread of pathological aggregates, we used adeno-associated virus serotype-1 (AAV1) vectors expressing an artificial microRNA to reduce α -syn (miR-SNCA).¹⁷⁻²⁰ Our results indicate that prophylactic silencing of α -syn expression in mice reduces susceptibility to motor impairments caused by synuclein pathology and validates α -syn knockdown as a potential gene therapy approach to block the cell-cell transmission of pathological α -syn in Parkinson's disease and related synucleinopathies.

Materials and methods

Study design

The objective of this study was to determine whether α -syn knockdown confers neuronal protection against synucleinopathy in mice. A single intracerebral injection of human MSA brain homogenate via the parietal lobe to the thalamus in mice causes a bilateral synucleinopathy, neuronal degeneration and profound motor deficits, whereas control, age-matched brain homogenates do not induce this pathology for up to a year post-inoculation.¹¹⁻¹⁴ The widespread α -syn pathology is composed of detergent-insoluble and protease-resistant phosphorylated α -syn, with preferential accumulation in midbrain and brainstem regions. Subsequent serial inoculation of healthy mice with brain homogenates derived from synucleinopathy-affected mice (MSA_{mo}) efficiently reproduces

the clinicopathological features, thereby providing a reliable murine model of synucleinopathy with predictable and progressive changes in protein aggregation and motor impairments. All inoculum used in this study was derived from brain homogenates from mice sacrificed at clinical disease endpoint (MSA_{mo}).

In our experimental paradigm, three-month old hemizygous transgenic M83 (TgM83^{+/-}) mice,²¹ which express human A53T-mutant α -syn under the control of the mouse prion protein promoter, were injected into the dorsal hippocampus with AAV1 vectors encoding either eGFP or miR-SNCA. One month later, the mice were injected with 1 μ g of MSA_{mo} inoculum to initiate the synucleinopathy. The animals were assessed regularly for changes in motor function until 150 days post-inoculation (dpi), when they were sacrificed, and brains were prepared for immunochemical and biochemical analyses. The sample size for the experiments was chosen based on our power analysis that indicated 14 animals per group (7M and 7F) would provide sufficient power for the behavioural tests and allow for a dropout of up to 10%. All biochemical and immunofluorescence analyses were replicated in at least two independent experiments with a minimum sample size of $n=4$. In addition, all the behaviour analyses and quantifications of phosphoserine129- α -syn (p-syn) pathology, and tyrosine hydroxylase (TH)-positive cell counts were scored by researchers blinded to the treatment group.

Mice

Homozygous A53T α -syn transgenic M83 mice were purchased from Jackson Laboratory (USA) and then crossed with C57/C3H.F1 mice to generate hemizygous M83 mice which were maintained on a 12 h light/12 h dark cycle with unlimited access to food and water. All animal experimental procedures were performed in compliance with guidelines set by the Canadian Council on Animal Care and the Animals for Research Act of Ontario under a protocol approved by the University Health Network Animal Care Committee.

Viral vectors

Recombinant AAV1 viral vectors were generated and characterized at Sanofi-Genzyme (Framingham, MA, USA). A targeting sequence that was previously shown to effectively target mouse and human SNCA mRNAs (5'-GCAGTGAGGCTTATGAAAT-3')²² was embedded into an artificial microRNA (miR) backbone and cloned into a previral vector as previously reported.²³ This plasmid was engineered to express the miR targeting SNCA (miR-SNCA) and an enhanced GFP (eGFP) reporter gene under the transcriptional control of a chicken β -actin (CBA) promoter (pSP70-CBA-eGFP). High-titre recombinant AAV1 serotype vectors encoding the miR-SNCA targeting sequence and control eGFP vector were generated. All

AAV vectors were designed to keep their distribution, transduction and expression consistent for the two transgenes (eGFP and miR-SNCA) by using the same serotype (AAV1), promoter (CBA), and parallel production and purification procedures from a single source (Sanofi-Genzyme). Briefly, the vectors were generated by triple-plasmid co-transfection of human 293 cells, and the recombinant virions were column purified as previously described.²⁴ The resulting titre of AAV1-CBA-eGFP was 8.82×10^{12} vector genomes (VG)/ml, and the titre of AAV1-CBA-miR- α -syn was 6.6×10^{12} VG/ml.

Stereotaxic injections

Two doses of either control (AAV1-CBA-eGFP) or test (AAV1-CBA-miR-SNCA) virus at a concentration of 1.25×10^8 VG/g per injection were unilaterally administered into the right hippocampus of 3-month-old Tg M83^{+/-} mice using a Hamilton micro syringe with a 30 G needle. The coordinates from Bregma: AP -2.1 mm; ML -1.5 mm; DV -1.7 mm and AP -1.75 mm; ML -1.5 mm; DV -2.3 mm were applied for the two injections. Thirty days later, the mice were anaesthetized and injected with 30 μ l of MSA_{mo} brain homogenate (1% w/v in 5% BSA) as previously described by Prusiner et al.¹¹ At 100 or 150 days-post MSA_{mo} inoculation, the mice were deeply anesthetized with sodium pentobarbital, transcardially perfused with phosphate-buffered saline and their brains isolated and processed for biochemical analysis or immunohistochemistry.

Behavioural analyses

Equal numbers of male and female mice in each treatment group were subjected to behaviour tests to assess motor function and all analyses were done by a researcher blinded to the treatment paradigm.

Vertical Screen test

A modification of the vertical grid test, the screen test was used to detect gait abnormalities and provide a sensitive measure of motor coordination. The mice were placed at the top of a vertical wire mesh, that was then tilted at an angle of 60 degrees to the surface. The number of steps and time taken to climb down were measured. A trial ended when the mouse reached the edge of the mesh or at the cut-off time of 60s and the average of three trials were recorded for each animal. The test was repeated once a week until the mice reached clinical disease endpoint or at 150 dpi, depending on which time-point came first.

Fixed-speed rotarod

To assess the animals' motor coordination and balance, a standard rotarod (Economex; Columbus Instruments, Columbus, OH) was used. Rotation was set at a constant speed of 12 revolutions per minute (rpm). Mice were

habituated to the rotarod for 4 days prior, performing 4 trials per day, each of 5 min duration, with a rest interval of 30 min between trials. On the fifth day, latency to fall off the rotarod was recorded and the sum of 4 trials was calculated.

Open field test

To evaluate spontaneous locomotor activity and anxiety-like behaviour at 100 dpi, the mice were individually placed in an open-field arena and their activity was monitored over 5 min with an overhead camera. Time spent walking, rearing and grooming were measured with OD log (Macropad Software, Yaraville, Victoria, Australia).

Immunohistochemistry

Mouse brains isolated for immunohistochemistry were post-fixed for 48 h in 4% paraformaldehyde (PFA) in 0.1 M phosphate-buffered saline (PBS; pH 7.4). After cryoprotection with 30% sucrose, horizontal sections (40 μ m) were collected using a sliding microtome. For immunostaining, free-floating sections were briefly rinsed with PBS, incubated in a blocking solution of 10% goat serum and 0.25% Triton X-100 in PBS for 1 h at room temperature. To visualize eGFP immunofluorescence, the sections were incubated with chicken anti-GFP antibody (ab13970, Abcam; 1:1000) overnight at 4°C, followed by incubation with secondary antibody goat anti-chicken IgG Alexa Fluor 488 (ab150169, Abcam; 1:2000). Nuclei were counterstained with DAPI (D9542, Sigma-Aldrich; 1:10 000). Additionally, the following antibodies were used to analyse α -syn expression and pathology: mouse anti-human α -syn Syn211 (32-8100, Invitrogen; 1:1000); rabbit anti-synaptophysin (ab52636, Abcam; 1:250), rabbit anti-phospho S129- α -syn EP1536Y (ab51253, Abcam; 1:1000), MJFR-14-6-4-2 (ab209538, Abcam; 1:500), LB509 (ab27766, Abcam; 1:1000). Autophagy was detected using mouse p62/SQSTM1 antibody (ab56416, Abcam; 1:500). To visualize neurons, two different NeuN antibodies (guinea pig ABN90, Millipore-Sigma; 1:500 or mouse MAB377, Millipore-Sigma; 1:300), and anti-TH (ab76442, Abcam; 1:1000) were used. To detect apoptotic cell death, terminal deoxynucleotidyl transferase-mediated dUTP-fluorescein nick-end labelling (TUNEL) (ab66110, Abcam) and cleaved caspase-3 immunostaining with rabbit anti-cleaved caspase-3 (9661S, Cell Signaling Technology; 1:500) were used. Inflammatory response was analysed by immunoreactivity to the astrocyte marker glial fibrillary acidic protein (GFAP) and the microglial marker Iba-1 as previously described,²⁵ followed by incubation with donkey anti-rabbit IgG Alexa Fluor 647 (711-605-152, 1:400; Jackson ImmunoResearch Laboratories) for Iba-1 and donkey anti-goat IgG Alexa Fluor 555 (ab150130, 1:400; Abcam) for GFAP for 2 h at room temperature.

For double labelling of dopamine transporter (DAT) and TH, the sections were incubated in blocking solution (5% donkey serum, 0.3% Triton X-100, PBS) for 1 h at

room temperature, followed by incubation with primary antibodies rat anti-DAT (MAB369, Millipore-Sigma; 1:200) and chicken anti-TH (ab76442, Abcam; 1:1000) overnight at 4°C. Following 3 washes with PBS, the sections were incubated with donkey anti-rat IgG Alexa Fluor 594 (712-585-150, Jackson ImmunoResearch Laboratories; 1:800) and donkey anti-chicken IgG Alexa Fluor 647 (703-605-155, Jackson ImmunoResearch Laboratories; 1:500) for 2 h at room temperature. Nuclei were counterstained with DAPI and following four washes with PBS, the sections were mounted using Prolong Diamond antifade mountant (ThermoFisher Scientific #P36961). For quantitative scoring of p-syn pathology, immunoreactive deposits in different brain regions were manually counted by a researcher blinded to the treatment cohort.

Proteinase K digestion

Forty micrometers free-floating cryosections were incubated with 20 μ g/ml Proteinase K (Sigma Aldrich) for 10 min at room temperature. Following three washes with PBS, immunohistochemistry was performed with the LB509 antibody as described above.

Analysis of dopaminergic neuronal markers

The HALO software (Indica Labs, Albuquerque, New Mexico) inbuilt cell-counting module was programmed to specifically mark and count cells that are both DAPI and TH positive, within the demarcated SNc, allowing for unbiased counting of neurons. The program generated output images showing each neuron that was counted, which was used to confirm that every TH-positive neuron was marked and that neurons were not counted twice. To analyse the number of dopaminergic neurons in the SN, 20 \times fluorescent images were taken from 4 specific depths (-3.96, -4.12, -4.28 and -4.44 mm of bregma) within the ipsilateral SN. The number of TH-immunoreactive cell bodies was counted using HALO image analysis software and the average cell-count within the ipsilateral hemisphere was calculated for each animal tested ($n=4$ /group). For quantification of striatal dopaminergic innervation, TH and DAT immunofluorescence within the ipsilateral striatum were captured at 20 \times magnification. The average fluorescence intensities from three separate fields, chosen within the same striatal regions for each animal, were measured using FIJI software and an average of the three regions was calculated per animal ($n=6$ /group).

Image acquisition

Images were acquired using a Zeiss LSM880 scanning confocal microscope coupled to a CCD camera (Zeiss Axio Observer.Z1, Carl Zeiss, Don Mills, Ontario,

Canada) and Zen software (Carl Zeiss). Image analysis was done using FIJI (NIH) and HALO (Indica Labs) image analysis software.

Biochemical analysis and Western blotting

Ten per cent (w/v) hippocampal, striatal and midbrain lysates were prepared as described previously.¹⁵ Detergent extracted α -syn was obtained using a two-step protein extraction protocol. Ten per cent midbrain lysates were incubated in detergent buffer [5% (v/v) Nonidet P-40, 5% (w/v) sodium deoxycholate in PBS] containing Pierce Universal Nuclease and Halt Phosphatase Inhibitor (Pierce) for 20 min on ice and clarified by centrifugation at 1000 \times g for 5 min at 4°C. The supernatant was carefully removed and treated with 1% Triton X-100 extraction detergent (150 mM NaCl, 20 mM Tris pH 7.5, 1% Triton X-100) containing protease inhibitors (Roche) for 30 min on ice. The samples were centrifuged at 100 000 \times g for 1 h at 4°C using a TLA-55 rotor (Beckman). The supernatant represented the Triton X-100 soluble α -syn fraction and the pellet, consisting of the Triton X-100 insoluble fraction, was dissolved in an equal volume of SDS-Urea buffer (20 mM Tris, 2% SDS, 8M Urea).

To quantify detergent extracted α -syn, the Triton X-100 soluble and insoluble fractions were boiled briefly in loading buffer and resolved by electrophoresis on a 12% SDS-polyacrylamide gel. Proteins were transferred to nitrocellulose membranes and fixed onto membranes by incubation with 0.4% PFA for 30 min at RT. The membranes were blocked with 5% (w/v) non-fat dry milk in Tris-buffered saline (TBS) with 0.01% Tween 20 (TBS-T) for 1 h and then probed overnight with the following primary antibodies: anti- α -syn (human specific Syn211-Life Technologies, 1:1000; species-nonspecific Syn1-BD BioSciences, 1:1000; murine specific α -syn D37A6-Cell Signaling Technology, 1:10 000), anti-Ser129-phosphorylated α -syn EP1536Y (Abcam, 1:2000), gamma-actin (Santa Cruz biotechnology, 1:10 000). Following 1 h incubation with horse radish peroxidase-conjugated secondary antibodies, chemiluminescence signal was obtained using the Amersham ECL detection kit (GE Healthsciences) and developed with the Odyssey Imaging system (LI-COR). Band intensities were quantified using Image Studio software (LI-COR) and normalized to loading controls in each lane.

Statistical analysis

All statistical analyses were performed using Prism 6.0 (GraphPad Software, San Diego, CA, USA) with a significance threshold of $P=0.05$. Data are presented as scatter plots with individual points and means. Quantification in all graphs were independently performed with a minimum sample number of $n=4$ per group for appropriate statistical analysis. Behavioural data were analysed by

two-way ANOVA. Pairwise *post hoc* comparisons applied Fisher's least significant difference (LSD) test, or Welch's *t*-tests, as appropriate. Differences between groups in expression and immunostaining experiments were assessed by unpaired Student's *t*-tests or Mann-Whitney test, where distributions were non-parametric.

Data availability

The authors confirm that the data supporting the findings of this study are available within the article and the [Supplementary material](#).

Results

miR-SNCA reduces α -syn expression in vivo

To test the ability of α -syn knockdown to protect against pathology and motor dysfunction in an aggressive model of α -syn pathology, we used hemizygous transgenic M83 (TgM83^{+/-}) mice, which express human A53T α -syn controlled by the mouse prion promoter.²¹ These mice age normally and without neurological deficits, but develop profound motor deficits and bilateral synucleinopathy following inoculation with MSA brain homogenates into the thalamus via the parietal lobe.¹¹ In contrast, brain homogenates from age-matched healthy controls fail to induce pathology for up to a year post-inoculation.¹¹⁻¹⁴ To avoid possible tissue damage and inflammation caused by injections into the thalamus prior to the α -syn seeding,²⁶⁻²⁹ which could confound the therapeutic benefits, we took advantage of known hippocampal connections with the thalamus ([Supplementary Fig. S1](#), Allen Brain project illustration) and the ability of AAV1 to undergo retrograde transport and anterograde transsynaptic exchange³⁰⁻³² to enable viral expression in the thalamus. Three-month-old TgM83^{+/-} mice received two unilateral injections of AAV1 vectors (1.25×10^8 viral genomes) into the dorsal hippocampi expressing either eGFP or microRNA-SNCA (miR-SNCA) targeting both human and murine α -syn ([Fig. 1A](#)). One month later, animals were inoculated in the thalamus with serially passaged, MSA-inoculum-derived mouse brain homogenate (MSA_{mo}), as described by Prusiner et al.^{11,12} At 100 dpi, robust eGFP immunofluorescence was detected in the ipsilateral hemisphere, extending from the dorsal hippocampus and surrounding corpus callosum, septum and thalamus, but not the mid-brain or cerebellum ([Fig. 1B-I](#)). In the contralateral hemisphere, only trace levels of eGFP expression in glia were observed within the cortex ([Fig. 1J](#)). This distribution indicates transport of virus from the injection site to the thalamus.

Next, the effect of miR-SNCA expression on α -syn levels was determined using immunofluorescence to assess the extent and distribution of α -syn knockdown

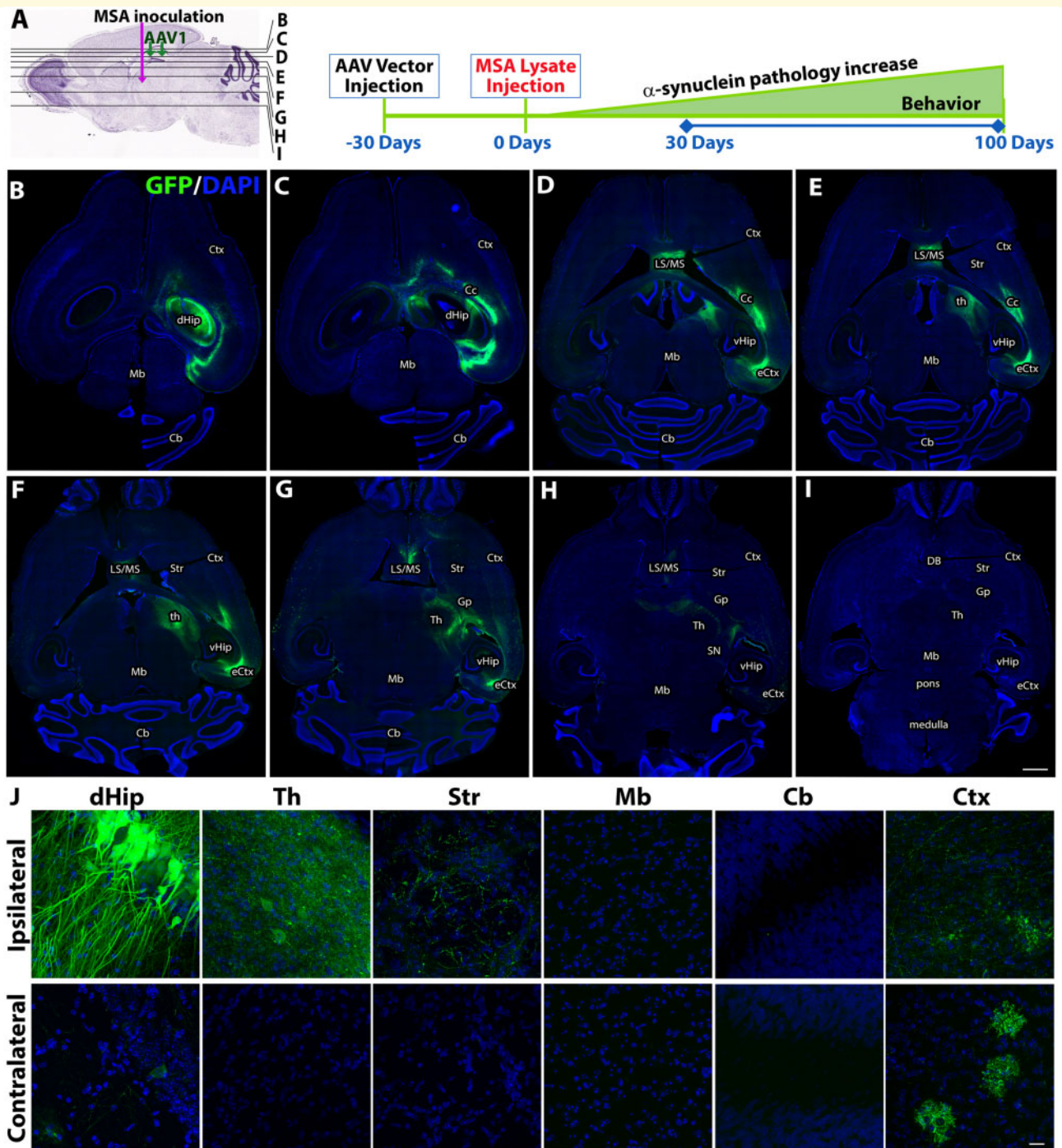


Figure 1 AAVI vector injection induces robust dorsoventral expression of transgenes. **(A)** Sagittal view of the mouse brain shows sites of virus injection and MSA inoculation. The black lines indicate axial planes of brain slices shown in panels **B–I**. Schematic overview of the study's experimental design is shown. **(B–I)** Axial brain sections from AAVI-eGFP injected TgM83^{+/-} mice depict eGFP expression (green) along the dorsoventral axis of the brain, including the dorsal (dHip) and ventral hippocampus (vHip), cortex (Ctx), entorhinal cortex (eCtx), corpus callosum (Cc), lateral and medial septal nucleus (LS/MS), striatum (Str), thalamus (Th), diagonal band (DB), midbrain (Mb), substantia nigra (SN) and cerebellum (Cb). Nuclei were counterstained by DAPI (blue). Scale bar: 500 μ m. **(J)** Higher magnification images of the same sections show viral transduction in neurons and nerve terminals in different brain regions. Scale bar: 20 μ m.

(Fig. 2A). α -Syn levels were normalized to the presynaptic protein synaptophysin to account for subtle anatomical variations in the regions of interest. Mice injected with

the miR-SNCA vector had reduced human α -syn immunoreactivity within the hippocampus and thalamus (–35% and –25%, respectively), as compared to mice

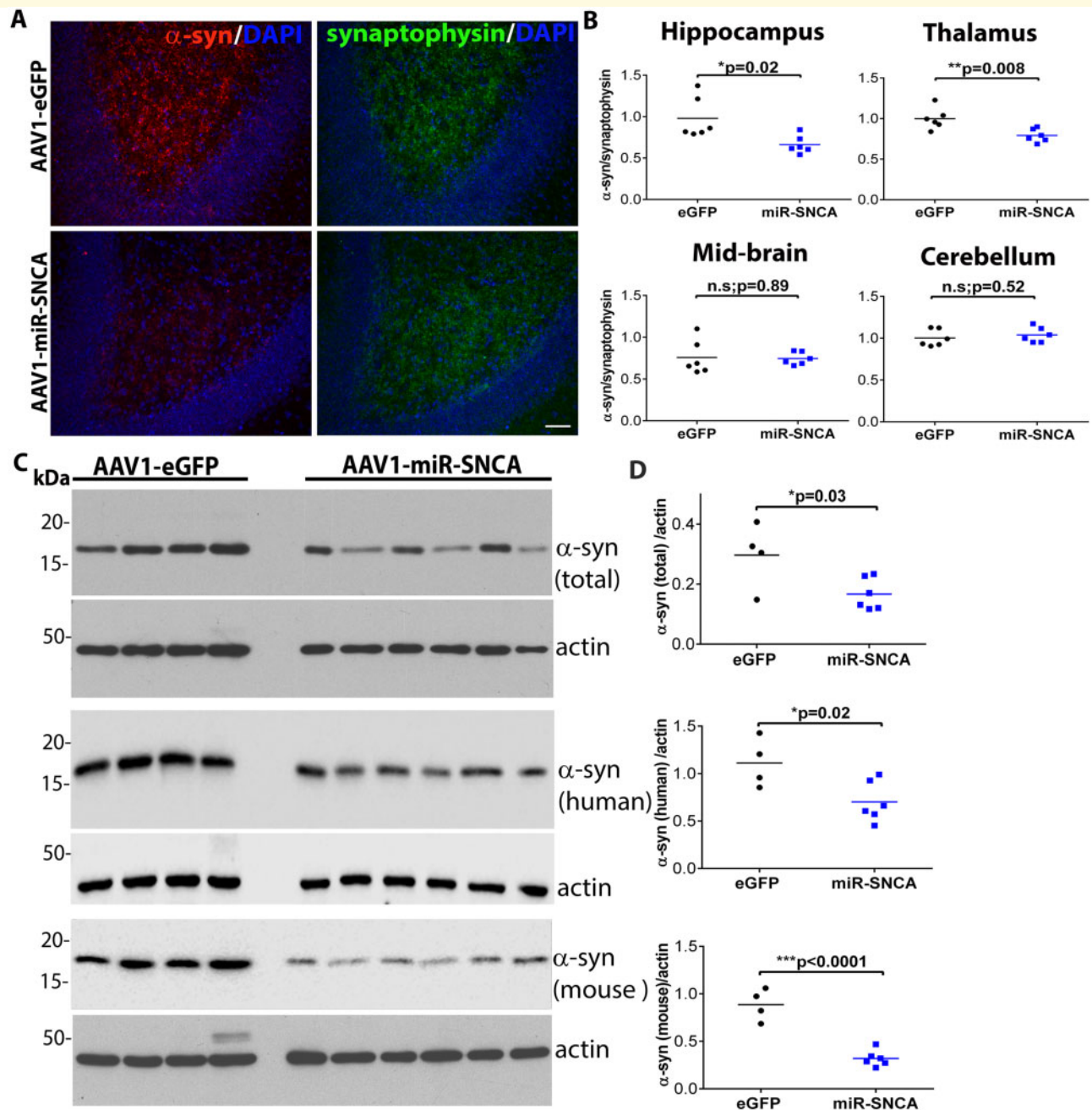


Figure 2 AAV1-mediated α -syn gene knockdown decreases α -syn expression. (A) Representative images show expression of human α -syn (Syn211, red) and synaptophysin (green) within the hippocampus of miR-SNCA and eGFP treated mice. Nuclei were counterstained with DAPI (blue). Scale bar: 100 μ m. (B) Quantification of the mean fluorescence intensities of α -syn staining in different brain regions are shown. Each point represents a single mouse ($n = 6$ /group; * $P \leq 0.05$, ** $P \leq 0.01$, unpaired t-test). (C, D) α -syn expression in the dorsal hippocampus of both groups of mice was analysed and quantified by western blotting using antibodies that detect total α -syn (Syn1 antibody), human-specific α -syn (Syn211 antibody) and murine-specific α -syn (D37A6 antibody). Each point represents a single mouse ($n = 4-6$ /group; * $P \leq 0.05$, *** $P \leq 0.001$, unpaired t-test).

that had received the control eGFP vector (Fig. 2B). In contrast, there was no observable effect on α -syn levels in more distal regions, such as the midbrain ($P = 0.89$) and cerebellum ($P = 0.51$; Fig. 2B). To confirm the knockdown

at the site of the AAV1 injections, α -syn expression was determined by Western blot analyses of hippocampal lysates using antibodies for total α -syn (-44% ; $P = 0.03$), as well as species-specific human transgenic (-37% ; $P = 0.02$), and

endogenous murine (-64% ; $P=0.0001$) α -syn (Fig. 2C and D).

miR-SNCA-mediated α -syn knockdown reduces behavioural deficits

We first measured changes in motor function by placing MSA_{mo}-inoculated mice on a vertical mesh screen and assessing their climb down from the screen as it was inclined to ~ 60 degrees, a modification of the vertical grid test.³³ The descending motor activity of mice that had received miR-SNCA remained consistent qualitatively and quantitatively (as determined by step coordination and the number of steps per second, respectively) over the testing period (Fig. 3A). In contrast, as the eGFP-expressing animals neared the expected clinical endpoint, their motor deficits were evident by pronounced hesitancy, poor hind-forelimb coordination, and an increasing propensity to fall off the grid, all marked by fewer overall steps (Supplementary movies M1, M2). We performed a two-way ANOVA to interpret the effect of α -syn

knockdown on the animals, over time. The performance of MSA_{mo}-inoculated animals, though not significantly affected by time post-injection ($F=0.13$, $DF=4,74$, $P=0.971$), was improved by miR-SNCA treatment ($F=10.53$, $DF=1,74$, $P=0.0018$). In this time course analysis, pairwise Welch's t -test comparisons were performed, as interpretation of the Fisher's t -statistic is confounded by high degrees of freedom. Our results indicated a protective effect of miR-SNCA at 65 days ($t=2.19$, $P=0.047$) and 86 days ($t=2.313$, $P=0.032$), but did not quite achieve significance at 100 days ($t=2.078$, $P=0.052$) after excluding an animal in the eGFP cohort that had reached clinical endpoint. Uninoculated mice were tested separately, over similar time points (Fig. 3D). Their performance was unaffected by miR-SNCA treatment ($F=1.33$, $DF=1,23$, $P=0.26$), or by time post-viral injection ($F=1.64$, $DF=3,23$, $P=0.209$) and pairwise Welch's t -comparisons confirmed no significant differences at any time point.

Next, to evaluate gross motor coordination and balance, both MSA_{mo}-inoculated and uninoculated mice were subjected to a fixed-speed rotarod test. Main effects

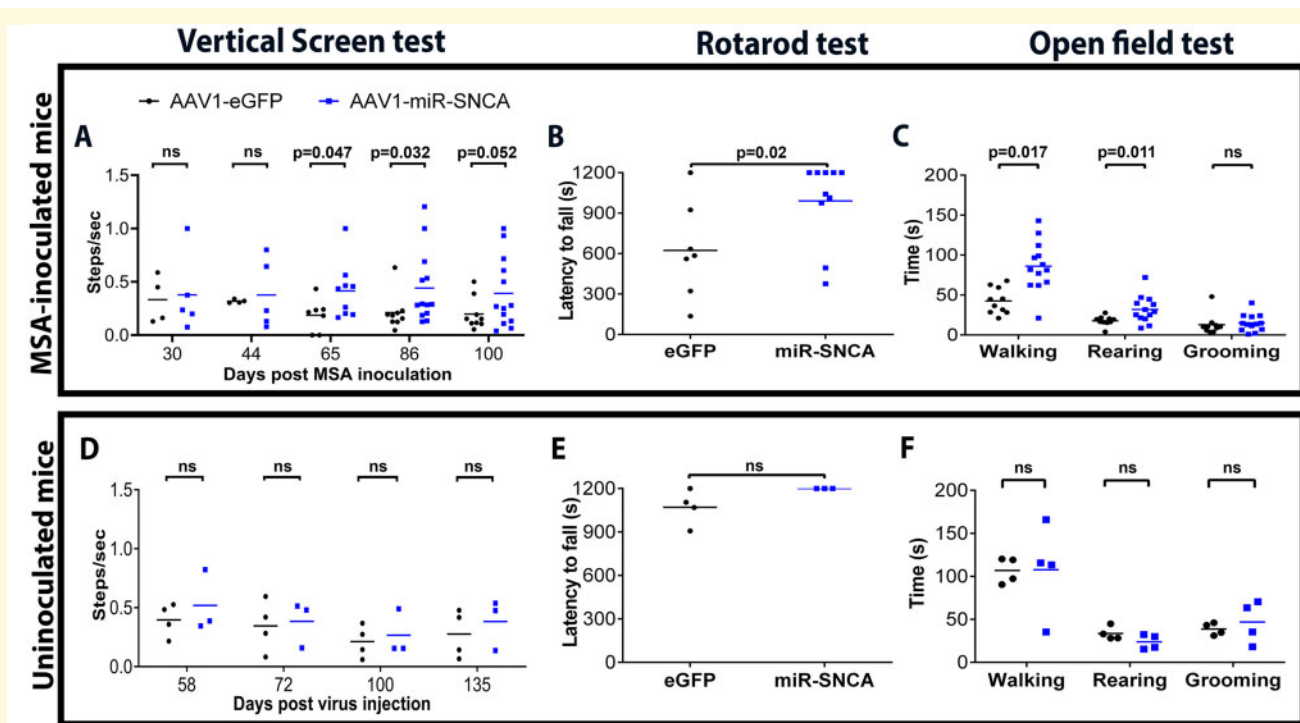


Figure 3 α -Syn knockdown rescues motor deficits associated with synucleinopathy. Motor behaviour of MSA_{mo}-inoculated and uninoculated mice that had been injected with either the AAV1-eGFP or AAV1-miR-SNCA vectors was analysed using three behaviour tests. (A) Vertical screen test: Data points represent the number of steps per second taken by the mice to move down the screen (Statistical analyses: Welch's t -test, $n=4-18$ /inoculated group). One animal within the AAV1-eGFP group reached disease endpoint at 65 dpi and was not included in the tests at 86 and 100 dpi. (B) Rotarod test: Latency to fall off the rotarod at 100 dpi are shown (Statistical analyses: two-way ANOVA and pairwise *post hoc* comparisons with Fisher's LSD test, $n=7-10$ /group). (C) Open-field test: Time spent by the mice in walking, rearing and grooming at 100 dpi are plotted (Statistical analyses: two-way ANOVA and pairwise *post hoc* comparisons with Fisher's LSD test, $n=14-18$ /group). (D-F) Data points represent motor behaviour of uninoculated mice in the vertical screen, rotarod and open field tests ($n=3-4$ /group). ns = not significant $P > 0.05$.

two-way ANOVA revealed impairment of rotarod performance with MSA_{mo} inoculation ($F=6.64$, $DF=1,21$, $P=0.0176$) and a beneficial effect of miR-SNCA treatment ($F=6.301$, $DF=1,21$, $P=0.0203$). Amongst the eGFP-expressing groups, MSA_{mo} inoculation increased impairment (Fisher's LSD $t=2.485$, $P=0.0219$). Consistent with the modified vertical grid test results, MSA_{mo}-inoculated mice expressing miR-SNCA performed markedly better on the rotarod at 100 dpi, than did their eGFP-expressing counterparts (999 ± 134 s versus 623 ± 134 s, respectively, Fisher's LSD $t=2.593$, $P=0.0174$) (Fig. 3B).

Mice were assessed in an open-field test to detect differences in spontaneous locomotor activity and exploratory behaviour (Fig. 3C). A reduction in walking was observed with MSA_{mo}-inoculation ($F=11.22$, $DF=1,28$, $P=0.0023$). Walking was improved by miR-SNCA treatment ($F=8.499$, $DF=1,28$, $P=0.0069$). Pairwise comparisons revealed a difference between MSA-inoculated and uninoculated mice that received the eGFP vector (Fisher's LSD $t=3.673$, $P=0.001$). In addition, MSA_{mo}-inoculated mice that received miR-SNCA walked more than did those receiving eGFP vector alone (Fisher's LSD $t=3.492$, $P=0.0017$).

Rearing activity was affected by the interaction of inoculation and viral vector administration ($F=5.55$, $DF=1,2$, $P=0.026$). However, significant main effects were not observed for either inoculation ($F=0.58$, $DF=1,27$, $P=0.4548$) or viral treatment ($F=0.19$, $DF=1,27$, $P=0.6696$) alone. Amongst mice that received control eGFP virus, rearing was decreased by MSA_{mo}-inoculation (Fisher's LSD $t=2.726$, $P=0.0394$). Treatment with the miR-SNCA prevented the decrease in rearing activity in MSA_{mo}-inoculated mice (Fisher's LSD $t=2.165$, $P=0.011$).

Finally, grooming was modulated by MSA_{mo} inoculation ($F=28.5$, $DF=1,28$, $P<0.0001$), but not by administration of the viral treatment ($F=0.6144$, $DF=1,28$, $P=0.4397$). MSA_{mo}-inoculated mice groomed less than did uninoculated animals. Pairwise comparison of eGFP-treated mice revealed a significant reduction associated with MSA_{mo}-inoculation (Fisher's LSD $t=3.277$, $P=0.0029$).

Taken together, these results demonstrate that even a modest ~25% reduction in α -syn levels at the site of inoculation can reduce synucleinopathy-linked motor deficits in mice.

Spreading α -syn aggregation is reduced by α -syn knockdown

In previous reports, the inoculation with MSA_{mo} brain homogenate induced widespread and bilateral neuronal pathology consisting of aggregated, phosphorylated α -syn, that extended caudally into the hindbrain, from the thalamus, hypothalamus, midbrain and brainstem. Although microgliosis and astrogliosis were also increased in areas with α -syn pathology, there was no evidence of α -syn pathology within those cell populations or in

oligodendrocytes.^{11–14} Therefore, as a measure of gene therapy efficacy, the number of phosphoserine 129- α -syn (p-syn) immunoreactive inclusions were quantified in different brain regions in both control and miR-SNCA treatment groups. At 100 dpi, there were significantly fewer p-syn positive inclusions in the α -syn knockdown group. This reduction in pathological α -syn extended to brain regions distal from site of the AAV1 injections, including the thalamus, subthalamic nucleus, midbrain, cerebellum and striatum (Fig. 4A and B, Supplementary Table 1).

In addition, we used four independent measures to confirm that the reduction in p-syn epitope corresponds to a decrease in misfolded, detergent-insoluble α -syn. First, a conformation-specific antibody MJFR-14-6-4-2 that specifically detects aggregated α -syn revealed markedly fewer α -syn inclusions in the miR-SNCA-treated mice relative to the eGFP control group (Fig. 5A). Second, the autophagy marker p62/SQTM, commonly found in Lewy bodies,^{34–36} co-localized with p-syn-positive inclusions in eGFP-treated mice, but not in the miR-SNCA treated mice, suggesting impaired autophagic flux in the animals with higher α -syn expression (Fig. 5B).^{37,38} Third, treatment of mouse brain tissues with proteinase K prior to immunostaining with the human specific α -syn antibody LB509 revealed a large number of proteinase K-resistant α -syn inclusions within eGFP-treated mice, but very few such deposits in the miR-SNCA-treated mice (Fig. 5C). Fourth, since pathological inclusions were more pronounced in the midbrain, we compared the levels of phosphorylated α -syn in midbrain homogenates. As shown in Fig. 5D, the recovery of p-syn was significantly reduced in the detergent-insoluble (–94%; $P=0.008$) and detergent-soluble (–48%; $P=0.004$) fractions in the miR-SNCA-treated group, in accord with the clinical and neuropathological features of the mice. Together, these results demonstrate that the partial α -syn downregulation significantly reduced the spread of pathological aggregated p-syn.

Dopaminergic cell survival and glial markers following α -syn knockdown

As with the other brain regions, the induction of striatal p-syn inclusions by the MSA_{mo} inoculum was inhibited by miR-SNCA expression (Supplementary Table 1). Despite a trend to lower total α -syn levels in striata of miR-SNCA versus eGFP-treated animals, the difference did not reach statistical significance (–24%, $P=0.09$; Fig. 6A), consistent with the weak eGFP expression in the caudal region of the striatum shown in Fig. 1J. However, to exclude the possibility raised by some reports,^{39–41} that a localized α -syn suppression might adversely influence TH-positive neurons in the substantia nigra (SN) and their projections to the striatum, we also assessed the integrity of the nigrostriatal dopaminergic pathway. In each region, relevant dopaminergic markers were evaluated from specific depths in the ipsilateral

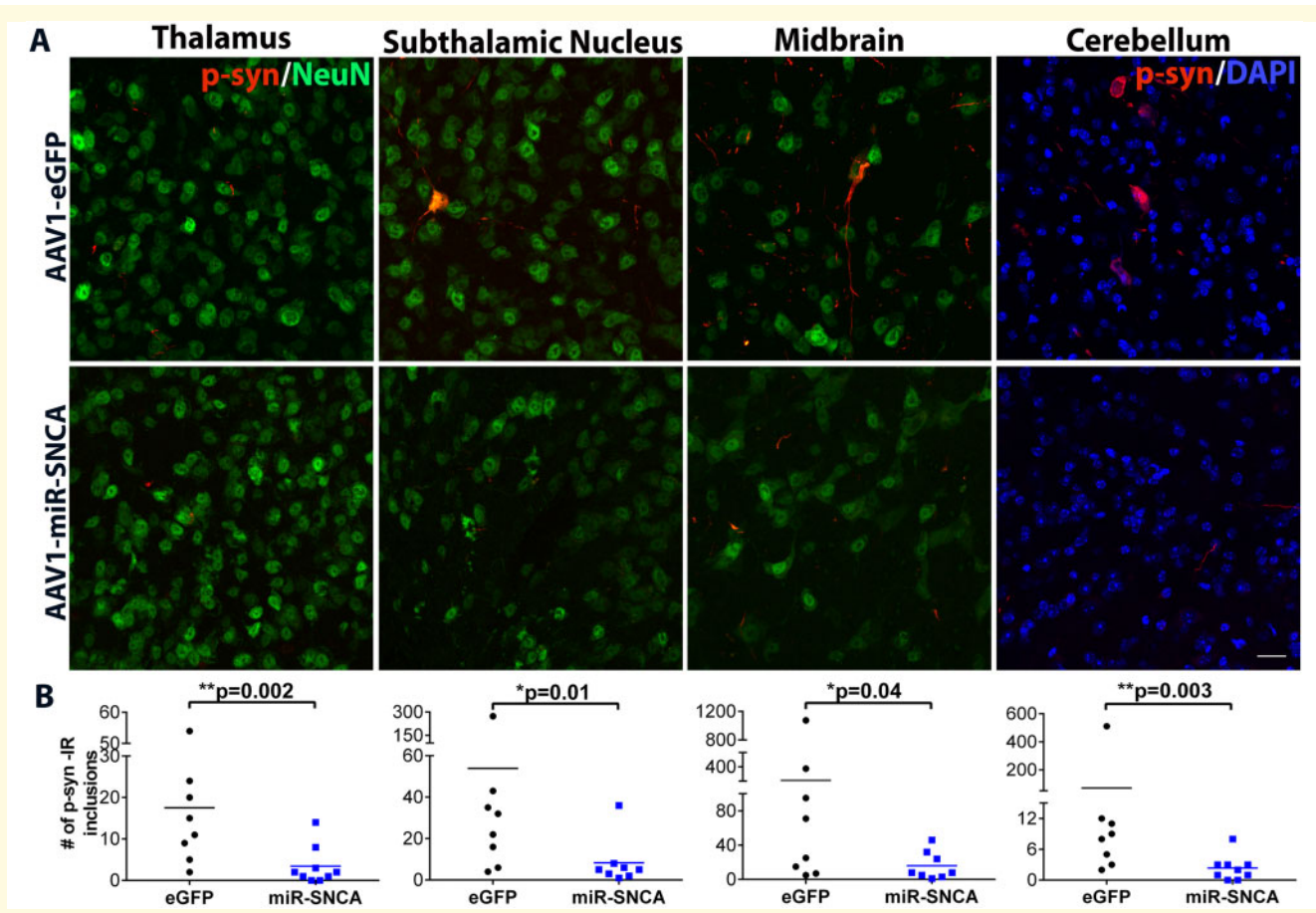


Figure 4 α -Syn knockdown mitigates the spread of phosphorylated- α -syn inclusions in MSA_{mo} -inoculated mice.

(A) Representative confocal images from MSA_{mo} -inoculated mice that had been injected with either the AAV1-eGFP or AAV1-miR-SNCA vectors show misfolded α -syn detected by phospho-Ser129- α -syn (p-syn, red) in the thalamus, sub-thalamic nucleus, midbrain and cerebellum. Nuclei were demarcated by counterstaining with NeuN (green) or DAPI (blue). Scale bar: 20 μ m. (B) Quantitative analysis of p-syn immunoreactive inclusions in different brain regions are shown. Each point represents a single mouse ($n = 8$ /group; * $P \leq 0.05$, ** $P \leq 0.01$, Mann-Whitney U-test).

hemisphere. There was no significant difference in the number of TH-immunoreactive nigral neurons between the eGFP and miR-SNCA expression groups, nor, as a measure of nigrostriatal dopaminergic innervation, in striatal TH or DAT expression, confirming that α -syn suppression in these mice did not induce dopaminergic degeneration (Fig. 6C and D).

As additional tests for potential detrimental consequences of α -syn knockdown, we assessed markers of apoptosis and glial activation in both treatment cohorts.⁴² At 100 dpi, we did not detect elevated terminal deoxynucleotidyl transferase dUTP nick end labelling (TUNEL)-positive cells in the hippocampus or midbrain in mice treated with either viral vector, relative to age-matched naïve, uninoculated TgM83^{+/-} mice (Fig. 7). Some increased TUNEL-positive staining was detected in the thalamus in both eGFP and miR-SNCA-treated groups compared to uninoculated mice, which we attribute to the lesion associated with the brain homogenate injection. Adjacent sections showed a corresponding increase in cleaved caspase-

3 staining in the thalamus (Supplementary Fig. 2). Interestingly, immunofluorescence of the microglial marker (Iba-1) suggested a small but significant decrease in microglial cell-density in the thalamus and midbrain in the miR-SNCA-treated group (thalamus: -22.5% in Iba-1 fluorescence intensity, $P = 0.03$; midbrain: -14.8% in Iba-1 fluorescence intensity, $P = 0.05$; Fig. 8). We did not observe any differences in GFAP-positive astrocyte density in any of the regions analysed. Overall, our results suggest that lowering α -syn levels did not induce neuronal loss, and that the consequent reduction in α -syn pathology is associated with reduced microglial infiltration.

Discussion

Permissive templating of unstructured proteins by their misfolded counterparts has emerged as a primary mechanism to explain spreading pathology in multiple

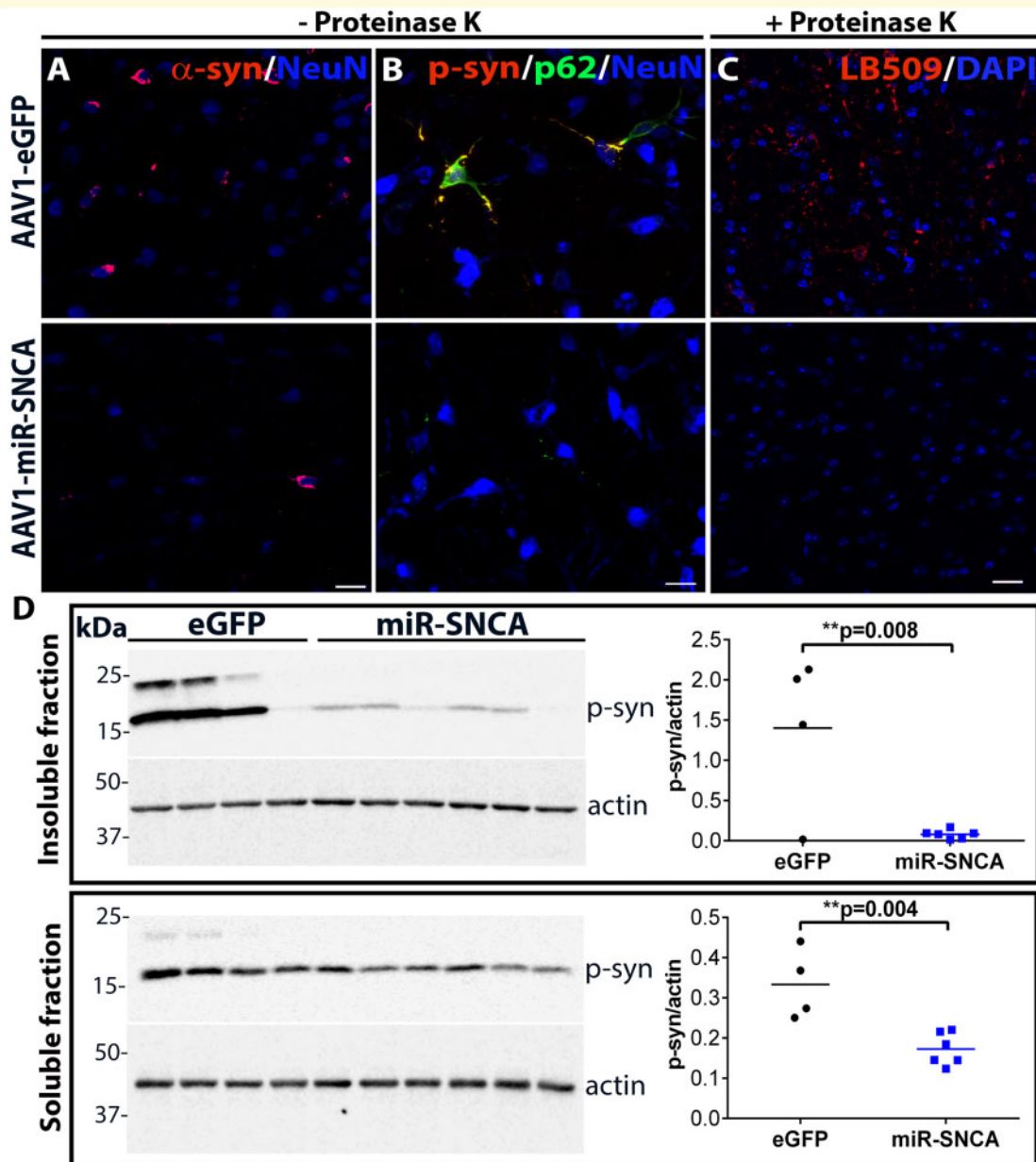


Figure 5 Viral gene therapy slows the progression of pathological aggregates. Pathological inclusions in the brains of MSA_{mo}-inoculated mice treated with either AAV1-eGFP or AAV1-miR-SNCA vectors were analysed by immunofluorescence using markers for aggregated α -syn. **(A)** The conformation-specific α -syn antibody, MJFR-14-6-4-2 (red) was used to detect misfolded α -syn. Neuronal nuclei were labelled with NeuN (blue). **(B)** Representative images show brain sections immunolabelled with the autophagy marker p62 (green), p-syn (red) and NeuN (blue). **(C)** To detect proteinase K resistant α -syn inclusions, free-floating tissues were subjected to mild proteinase K digestion prior to labelling with the human-specific α -syn antibody LB509 (red) and DAPI (blue). Signal intensities of the red channel was enhanced equally in both eGFP and miR-SNCA panels to enable better visualization of inclusions. Scale bars: 20 μ m. **(D)** Levels of phosphorylated α -syn in the detergent-soluble and insoluble fractions of mid-brain lysates were analysed by western blotting using the p-Ser129- α -syn (p-syn) antibody. Quantification of p-syn levels in the two fractions are shown. Each point represents a single mouse ($n = 4-6$ /group; ** $P \leq 0.01$, unpaired t-test).

neurodegenerative disorders.⁴³ The prion-like spread of α -syn along neuronal pathways has been amply demonstrated in multiple *in vitro* and *in vivo* models of synucleinopathy induced by seeding with α -syn fibrils.⁴⁴ Key cellular pathways predicted to regulate the kinetics of the spreading pathology include the internalization of extracellular seeds by recipient cells, the intracellular expansion of

misfolded α -syn exacerbated by oxidative stress, impairments in autophagy-lysosomal pathways and interaction with native α -syn, and the secretion of α -syn templates with newly acquired pathogenic structure.⁴⁵ Uncertainties regarding the mechanisms of entry and exit of α -syn seeds have thus far precluded their usefulness as therapeutic targets. Therefore, current approaches to limit α -syn

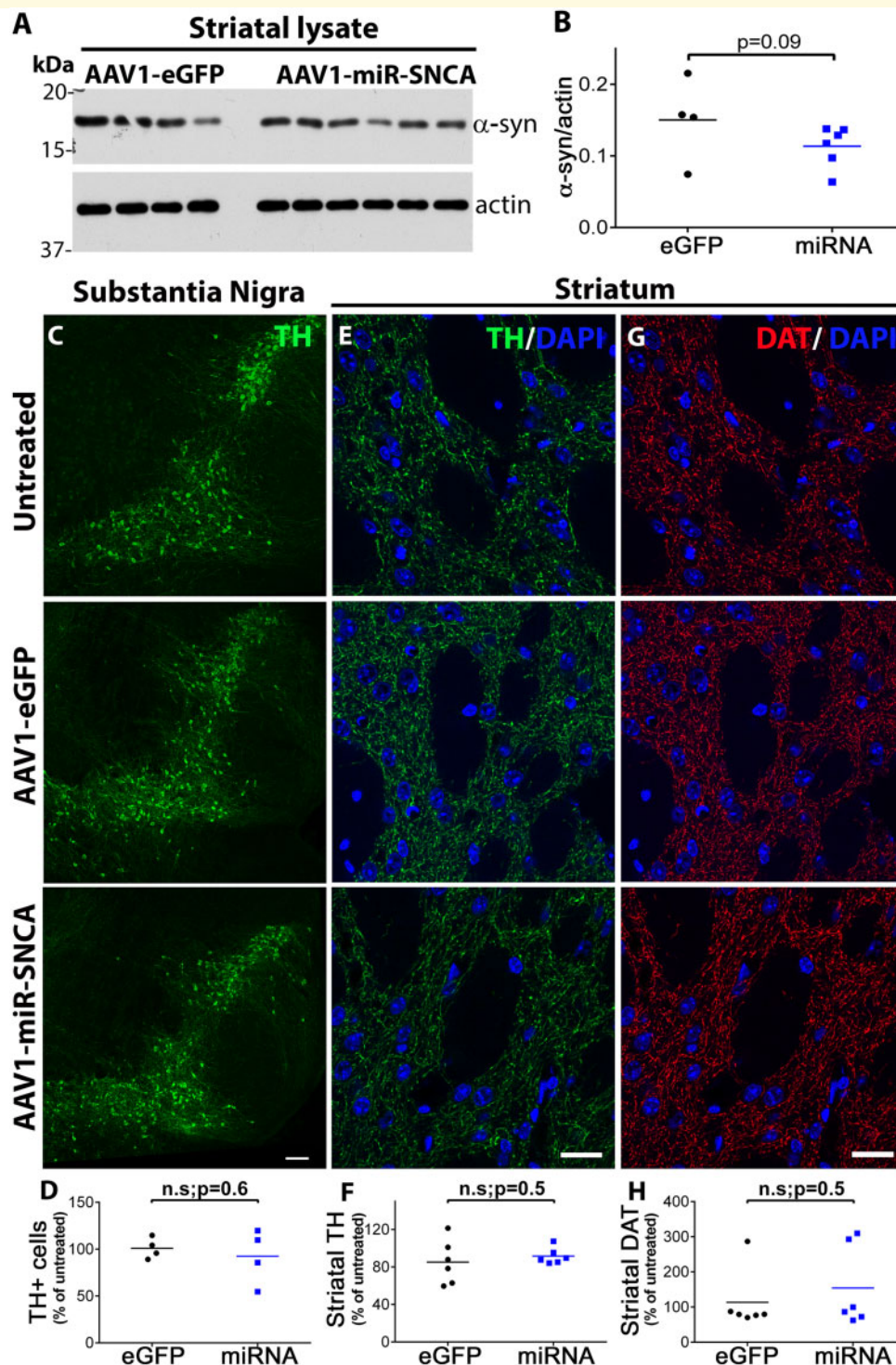


Figure 6 Nigrostriatal dopaminergic markers are not affected by α -synuclein knockdown. (A, B) The effect of hippocampal transgene delivery on striatal α -syn expression was quantified by western blotting using an antibody that detects total α -syn (Syn I antibody). Each point represents a single mouse ($n = 4$ –6/group, Mann–Whitney U-test). (C, D) To test if transgene expression in the striatum causes dopaminergic degeneration, the number of TH immunoreactive cells within the substantia nigra (SN) were counted. Representative images show TH-positive cells in the ipsilateral SN of untreated mice as well as eGFP and miR-SNCA treated MSA_{mo}-inoculated mice. The graph represents the average number of TH-positive cells counted from 4 specific depths (–3.96, –4.12, –4.28 and –4.44 mm of bregma) in the ipsilateral SN. Scale bar: 100 μ m ($n = 4$ /group, unpaired *t*-test). (E–H) Dopaminergic striatal innervation was measured by quantifying TH (green) and dopamine transporter (DAT, red) immunoreactivity in the striatum. Nuclei were counterstained with DAPI (blue). Graphs represent the mean TH and DAT immunofluorescence intensities in the ipsilateral striatum of untreated as well as eGFP and miR-SNCA treated synucleinopathy mice. Scale bar: 20 μ m. Each point represents a single mouse ($n = 6$ /group, unpaired *t*-test).

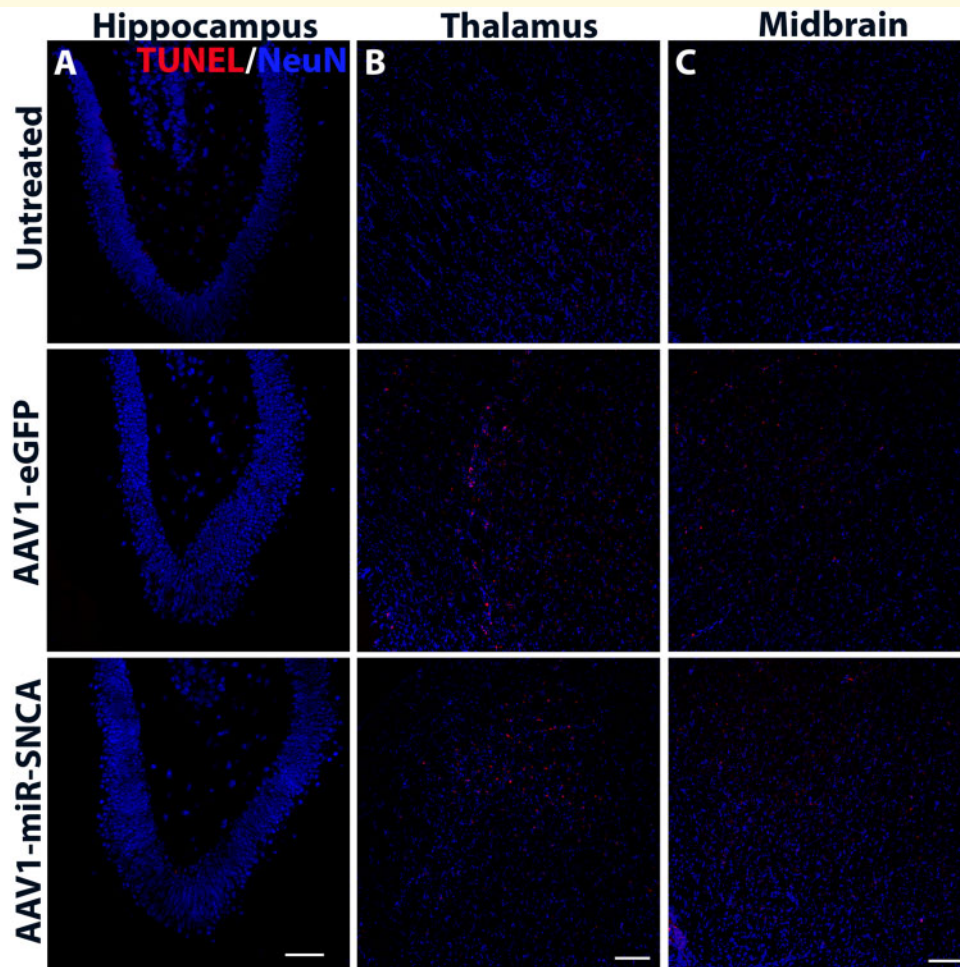


Figure 7 AAV1-mediated α -syn knockdown does not induce cell death. (A–C) Brains from eGFP and miR-SNCA treated MSA_{mo}-inoculated mice as well as untreated mice were analysed for apoptotic cell death using TUNEL staining. Representative confocal images of the hippocampus, thalamus and midbrain are shown with TUNEL positive cells labelled in red. Signal intensity of the red channel was enhanced equally across the panels to enable better visualization of TUNEL-positive cells. Neuronal nuclei are stained with NeuN (blue). Scale bar: 100 μ m.

pathology have focussed on reducing either the extracellular seeds or the intracellular α -syn substrate.

In this study, we tested whether α -syn knockdown using virus-encoded miR-SNCA can prevent the clinicopathological features in mice with rapid and progressive synucleinopathy induced by a single intracerebral injection of serially-passaged MSA_{mo} inoculum. Stereotaxic injections of control AAV1-eGFP vectors into the hippocampus induced robust eGFP expression within the hippocampus and surrounding corpus callosum, and thalamus, but not the midbrain, pons or cerebellum. In accord, in animals that received AAV1-miR-SNCA, hippocampal α -syn expression was reduced \sim 50%, as determined by immunofluorescence and immunoblotting, and in the thalamus by 25%, while there was no observable reduction in regions distal to the virus injection, such as the midbrain and the cerebellum. Based on previous studies, intracerebral injection of MSA_{mo} brain homogenate in TgM83^{+/-} mice induces a bilateral synucleinopathy that spreads caudally into the brainstem and results in progressive neurological

disease at 100–150 dpi that includes bradykinesia, impaired motor coordination, and eventual hindlimb paralysis.^{11,12}

Using this paradigm to compare between animals receiving AAV1 vectors expressing either control eGFP or miR-SNCA, our study provides several lines of evidence indicating that down-regulation of α -syn can mitigate the development of synucleinopathy. First, three tests of motor function (vertical grid, rotarod, and open field) showed that MSA_{mo}-injected animals expressing miR-SNCA maintained motor function over the test period, in contrast to progressive motor dysfunction in eGFP-expressing mice. Second, the rescue of motor function in the miR-SNCA cohort corresponded with significantly fewer p-syn-positive neurons in all brain regions analysed, a key pathological feature of synucleinopathy brains. Third, miR-SNCA-treated animals developed fewer proteinase K-resistant α -syn inclusions and epitopes recognized by an antibody specific for misfolded α -syn, confirming that lower α -syn levels were successful in preventing the accumulation of misfolded α -syn. Finally, the recovery of p-syn in

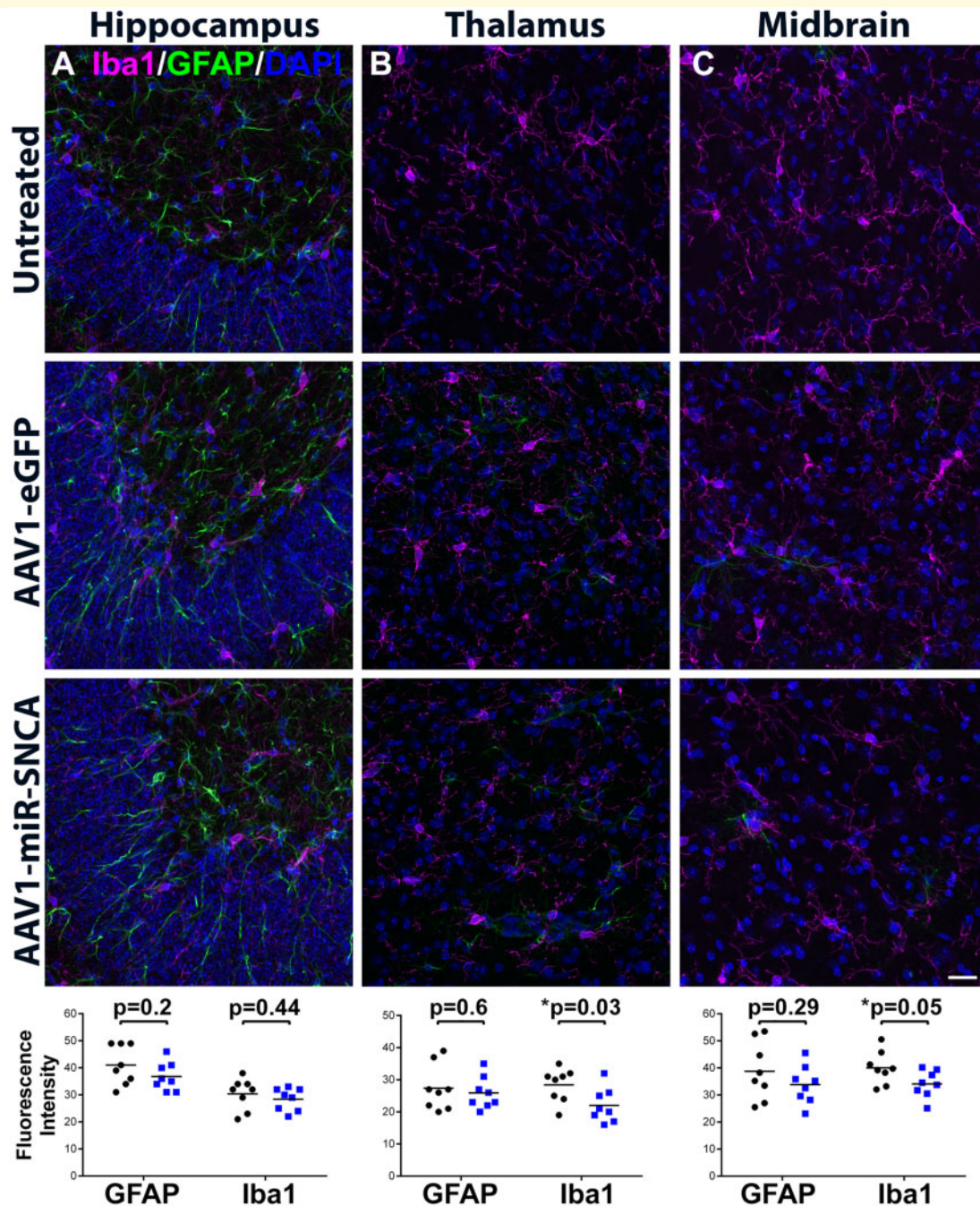


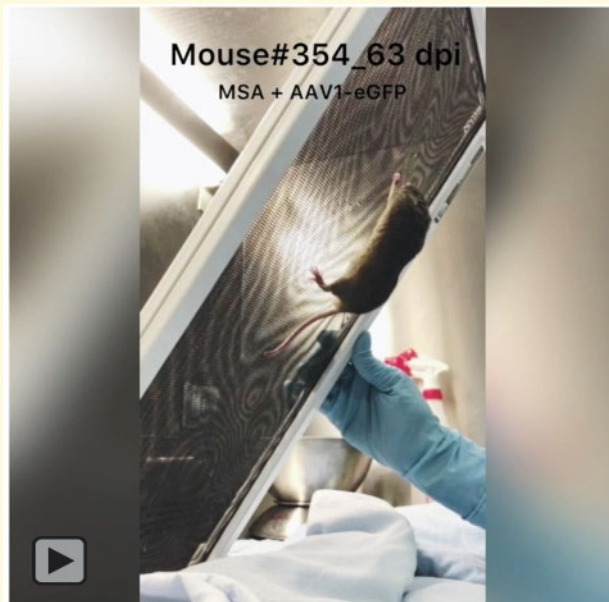
Figure 8 α -Synuclein knockdown does not induce a glial inflammatory response. (A–C) To test if AAV1 vector delivery causes neuroinflammation in our treatment paradigm, tissue sections from untreated mice as well as eGFP and miR-SNCA treated MSA_{mo}-inoculated mice were immunolabelled with the microglial marker Iba-1 (magenta) and glial fibrillary acidic protein (GFAP, green). Nuclei were labelled with DAPI (blue). Each point quantifying fluorescence intensity represents data from a single mouse ($n = 8$, unpaired t-test). Scale bar: 20 μ m.

detergent-soluble and -insoluble fractions of brain homogenates was markedly reduced by miR-SNCA treatment.

The observed co-localization of p62/SQTM with p-syn-positive inclusions in eGFP-treated mice indicates dysregulation of the autophagy-lysosomal pathway,⁴⁶ which was not observed in miR-SNCA-treated mice. Overexpression of α -syn can impair autophagy, lysosomal and proteasomal function,^{47–50} and conversely, inhibition of autophagy can

lead to enhanced exocytosis and spreading of α -syn species.^{51,52} Thus, the miR-SNCA-induced knockdown may suppress the aberrant reciprocal relationship between α -syn pathology and autophagy-lysosomal dysfunction, as implied by the reduced p62/SQTM accumulation.

Notably, the rescue of α -syn pathology also occurred in regions distal to the site of AAV1 injection, such as the midbrain and cerebellum, where neurons were not



Movie M1 Motor function of MSAmo-inoculated and AAV1-eGFP treated mouse in modified vertical grid test.

An AAV-eGFP treated animal performing on the vertical grid test at 63 days post MSAmo-inoculation. The motor deficits were evident by pronounced hesitancy, poor hind-forelimb coordination, and an increasing propensity to fall off the grid, all marked by fewer overall steps.



Movie M2 Motor function of MSAmo-inoculated and AAV1-miR-SNCA treated mouse in modified vertical grid test.

An AAV-miRNA-SNCA treated animal performing on the vertical grid test at 63 days post MSAmo-inoculation. The motor activity remained normal, both qualitatively and quantitatively (as determined by step coordination and the number of steps per second, respectively) over the testing period. Motor function of MSAmo-inoculated and AAV1-miR-SNCA treated animal performing on the vertical grid test at 63 days post MSAmo-inoculation. The motor activity remained normal, both qualitatively and quantitatively (as determined by step coordination and the number of steps per second, respectively) over the testing period.

transduced by AAV1 and total α -syn levels unaffected. These data suggest that local suppression of α -syn proximal to the site of the initial pathology (the thalamus) was sufficient to limit the ability of the α -syn fibrils in the MSAmo inoculum to template and propagate the pathology into other brain regions along connected neuronal pathways.^{53–55} Previous studies suggest that pathology is comprised of mainly human α -syn and that contribution of murine α -syn in this mouse model is negligible. The human Tg α -syn levels in these hemizygous animals are 3.3-fold higher than the endogenous mouse α -syn²¹ and human α -syn aggregates are more potent in inducing aggregation of human α -syn than of mouse α -syn.^{9,56} Also, using human and mouse-specific antibodies, we recently reported that inoculated TgM83 brain lysates contain abundant detergent-insoluble, protease-resistant human α -syn, but no detectable mouse α -syn with corresponding properties.¹⁵

Acute loss of α -syn expression has been implicated in dopaminergic cell death.^{39–41} Although we did not directly target the nigrostriatal pathway, α -syn levels in dissected striatal tissue from miR-SNCA-treated animals trended lower ($P=0.09$), possibly due to some AAV1 expression detected at the periphery of the striatum. We found no adverse changes in nigral or striatal dopaminergic markers in mice with α -syn knockdown. Our results are consistent with other studies that have evaluated α -syn knockdown using various strategies.^{16,22,25,57–62} We previously showed that 40–60%

α -syn reduction using AAV9-expressed shRNA did not induce dopaminergic or other neuronal loss in mice expressing only human α -syn.²⁵ Similarly, silencing of endogenous α -syn production in adult rodents did not cause nigrostriatal neurodegeneration; instead, it protected against toxin-induced cell death.²² Transient α -syn reduction following administration of antisense oligonucleotides (ASOs) also rescued α -syn pathology induced either by α -syn overexpression or fibril seeding in mice, with efficacy and safety replicated in non-human primates.^{16,60–65} Markers of apoptotic cell death or glial activation were also not increased by α -syn knockdown in our study, and conversely, there was some reduction in microglia/macrophage marker Iba-1 in the thalamus and midbrain following miR-SNCA treatment, two brain regions that accumulated abundant p-syn pathology following MSAmo inoculation. These results are in line with reports showing microglial activation in response to α -syn aggregation,^{66,67} which can lead to a further increase in α -syn aggregation through post-translational modifications^{68,69} and enhanced α -syn spreading.⁷⁰ Our findings suggest that minimizing α -syn self-assembly by limiting α -syn substrate can dampen the associated inflammatory responses.

Importantly, the main finding in this study that a ~25–50% reduction in α -syn is sufficient to confer protection against motor deficits and spreading pathology provides optimism for current efforts to lower α -syn levels in human synucleinopathies. Multiple clinical trials are evaluating a variety of approaches to decrease brain α -syn, including passive and active immunization to sequester extracellular α -syn or impede its interneuronal transfer.^{71–74} While some antibodies have shown promising pre-clinical results, target engagement in humans is significantly constrained by poor blood-brain barrier (BBB) penetration, generally <0.5% when comparing serum and CSF immunoglobulin ratios.^{75,76} Additional pharmacological strategies under consideration involve inhibition of α -syn transcription via the β 2-adrenoreceptor, modulation of autophagy, or by enhancing the activity of lysosomal enzymes, such as glucocerebrosidase.^{77–81} Non-viral gene regulation with ASOs to preferentially degrade α -syn mRNA also shows promise,^{16,60–62,82} although ASO stability and transient efficacy necessitates repeat administration. Conversely, AAV-based gene therapy can induce stable, long-lasting up- or down-regulation of target proteins. Furthermore, the neuronal tropism and low toxicity of AAVs make them an attractive vehicle to encode therapeutics for treating human proteopathies. Previous phase I/II clinical trials for Parkinson's disease using AAVs to express growth factors or enzymes involved in dopamine biosynthesis showed good safety profiles, despite the short-lasting and limited therapeutic efficacy.⁸³ Arguably, these trials were evaluated in small patient cohorts with mid- to late-stage disease and did not address underlying α -syn aggregation. Our results suggest that early localized intervention can reduce the transmission of α -syn pathology from fibril-seeded brain regions. Future combinatorial gene therapy approaches, where α -syn knockdown is supplemented with growth factor and/or dopamine modulating strategies, offer the exciting possibility to reduce pathological α -syn and achieve symptomatic relief by maintaining cellular health and/or neurotransmission.

Limitations

There are some limitations to the current study. For example, we initiated α -syn knockdown prior to the induction of pathology, an option not available in clinical settings. Although AAV1 pre-treatment prevented the severe MSA_{mo}-induced pathophysiology, the rapid decline to clinical endpoint within 3–5 months poses a challenge for assessing post-inoculation rescue. In contrast, human synucleinopathies develop over years to decades, offering a longer therapeutic window. Indeed, the use of ASO in slower, milder disease models suggest transient disease-modifying benefits after pathology is triggered.^{62,63,65,84,85} While accurate pre-clinical diagnosis of idiopathic Parkinson's disease remains a challenge, recent advances in ascribing predictive disease risk based on prodromal

symptoms and other biomarkers could facilitate earlier and more targeted treatment regimens.^{86,87}

The current study relies on the increased aggregation kinetics of a rare Parkinson's disease-linked α -syn mutant.⁸⁸ However, it should be noted that the aggregates generated in A53T α -syn transgenic mice reproduce the biological and biochemical characteristics of those in MSA inoculum,¹⁴ suggesting that seeding properties are preserved. Our demonstration that suppressing α -syn with AAV1-miRNA-SNCA mitigates transmission of α -syn pathology and motor deficits is also in line with multiple clinical observations that link α -syn levels and seeding to the severity of Parkinson's disease pathology. For example, elevated α -syn expressed by SNCA gene multiplications cause familial Parkinson's disease⁸⁹ and α -syn pathology develops in healthy foetal cells grafted into Parkinson's disease brains.^{90,91}

Lastly, MSA-inoculation in TgM83^{+/-} mice does not cause glial inclusions,^{11,12} a hallmark of MSA, and it remains unknown whether AAV1-miR-SNCA can ameliorate α -syn pathology in this cell population based on the current study. Other mouse models engineered for α -syn pathology in oligodendrocytes could be used to answer this question,^{92–94} which may also require a viral vector optimized for glial expression.⁹⁵

Conclusions

This study provides proof-of-concept for viral-mediated α -syn suppression as a treatment for synucleinopathies. The recognition that early Lewy pathology can develop within brainstem nuclei in Parkinson's disease^{96–98} and is manifested clinically as non-motor prodromal symptoms, including gastric and sleep disturbances,^{87,99} identifies the initial brain regions for targeting the α -syn knockdown. We previously reported non-invasive delivery and expression of α -syn gene silencing vectors in multiple mouse brain regions using transcranial MRI-guided focused ultrasound combined with intravenous microbubbles to transiently increase BBB permeability.²⁵ The importance of this emerging technology is further underscored by successful Phase I clinical trials in Alzheimer's disease and Parkinson's disease patients that support the feasibility and safety of BBB opening with low intensity focal sonication.^{100,101} With ongoing improvements to vector design and CNS delivery, combinatorial gene therapies targeting cell survival and α -syn may offer long-lasting benefits by specifically targeting affected neuronal pathways implicated by prodromal disease symptoms, and which could mitigate further transmission of synucleinopathy.

Supplementary material

Supplementary material is available at *Brain Communications* online.

Acknowledgements

S.M. and A.T. wrote the first draft, and all authors edited the manuscript; A.T., S.M., I.A., J.C.W., P.E.F., H.T.J.M., S.P.S. and L.S.S. designed the experiments; S.M., R.H.K., F.N., K.X., T.L. and Y.A.F. performed the experiments.

Funding

This work was funded by the Canadian Institutes of Health Research (CIHR) operating grants to A.T. (PJT148736), I.A. (FRN166184, FRN168906) and P.E.F. (PJT173497), and Canada Research Chairs Program to IA and JCW. Fellowship/studentship support was provided to S.M. (Edmond J. Safra Fellowship), R.H.K. (Canadian Alzheimer Society Research Program Postdoctoral Fellowship #19-10 and Carlsberg Foundation Internationalisation Stipend #CF20-0379), F.N. (Queen Elizabeth II Graduate Scholarship in Science and Technology Program), K.X. (Frederick Banting and Charles Best Canada Graduate Scholarship GSD 152271).

Competing interests

S.P.S. is a Sanofi employee and stockholder.

References

- Spillantini MG, Goedert M. The alpha-synucleinopathies: Parkinson's disease, dementia with Lewy bodies, and multiple system atrophy. *Ann N Y Acad Sci*. 2000;920:16–27.
- Snead D, Eliezer D. Alpha-synuclein function and dysfunction on cellular membranes. *Exp Neurol*. 2014;23(4):292–313.
- Abeliovich A, Gitler AD. Defects in trafficking bridge Parkinson's disease pathology and genetics. *Nature*. 2016;539(7628):207–216.
- Burre J, Sharma M, Sudhof TC. Cell biology and pathophysiology of alpha-synuclein. *Cold Spring Harb Perspect Med*. 2018; 8(3):a024091.
- Desplats P, Lee HJ, Bae EJ, et al. Inclusion formation and neuronal cell death through neuron-to-neuron transmission of alpha-synuclein3. *Proc Natl Acad Sci USA*. 2009;106(31):13010–13015.
- Frost B, Diamond MI. Prion-like mechanisms in neurodegenerative diseases. *Nat Rev Neurosci*. 2010;11(3):155–159.
- Lashuel HA, Overk CR, Oueslati A, Masliah E. The many faces of alpha-synuclein: From structure and toxicity to therapeutic target. *Nat Rev Neurosci*. 2013;14(1):38–48.
- Chu Y, Kordower JH. The prion hypothesis of Parkinson's disease. *Curr Neurol Neurosci Rep*. 2015;15(5):28.
- Luk KC, Kehm V, Carroll J, et al. Pathological alpha-synuclein transmission initiates Parkinson-like neurodegeneration in non-transgenic mice. *Science*. 2012;338(6109):949–953.
- Rey NL, Petit GH, Bousset L, Melki R, Brundin P. Transfer of human alpha-synuclein from the olfactory bulb to interconnected brain regions in mice. *Acta Neuropathol*. 2013;126(4):555–573.
- Watts JC, Giles K, Oehler A, et al. Transmission of multiple system atrophy prions to transgenic mice. *Proc Natl Acad Sci U S A*. 2013;110(48):19555–19560.
- Prusiner SB, Woerman AL, Mordes DA, et al. Evidence for alpha-synuclein prions causing multiple system atrophy in humans with parkinsonism. *Proc Natl Acad Sci U S A*. 2015; 112(38):E5308–E5317.
- Dhillon JS, Trejo-Lopez JA, Riffe C, et al. Comparative analyses of the in vivo induction and transmission of alpha-synuclein pathology in transgenic mice by MSA brain lysate and recombinant alpha-synuclein fibrils. *Acta Neuropathol Commun*. 2019;7(1):80.
- Woerman AL, Oehler A, Kazmi SA, et al. Multiple system atrophy prions retain strain specificity after serial propagation in two different Tg(SNCAA53T) mouse lines. *Acta Neuropathol*. 2019; 137(3):437–454.
- Lau A, So RWL, Lau HHC, et al. alpha-Synuclein strains target distinct brain regions and cell types. *Nat Neurosci*. 2020;23(1): 21–31.
- Luna E, Decker SC, Riddle DM, et al. Differential alpha-synuclein expression contributes to selective vulnerability of hippocampal neuron subpopulations to fibril-induced toxicity. *Acta Neuropathol*. 2018;135(6):855–875.
- Hadaczek P, Stanek L, Ciesielska A, et al. Widespread AAV1- and AAV2-mediated transgene expression in the nonhuman primate brain: Implications for Huntington's disease. *Mol Ther Methods Clin Dev*. 2016;3:16037.
- Kim S, Moon GJ, Oh YS, et al. Protection of nigral dopaminergic neurons by AAV1 transduction with Rheb(S16H) against neurotoxic inflammation in vivo. *Exp Mol Med*. 2018;50(2):e440.
- Wang D, Tai PWL, Gao G. Adeno-associated virus vector as a platform for gene therapy delivery. *Nat Rev Drug Discov*. 2019; 18(5):358–378.
- Hudry E, Vandenberghe LH. Therapeutic AAV gene transfer to the nervous system: A clinical reality. *Neuron*. 2019;101(5):839–862.
- Giasson BI, Duda JE, Quinn SM, Zhang B, Trojanowski JQ, Lee VM. Neuronal-synucleinopathy with severe movement disorder in mice expressing A53T human alpha-synuclein. *Neuron*. 2002; 34(4):521–534.
- Zharikov AD, Cannon JR, Tapias V, et al. shRNA targeting alpha-synuclein prevents neurodegeneration in a Parkinson's disease model. *J Clin Invest*. 2015;125(7):2721–2735.
- Stanek LM, Sardi SP, Mastis B, et al. Silencing mutant huntingtin by adeno-associated virus-mediated RNA interference ameliorates disease manifestations in the YAC128 mouse model of Huntington's disease. *Hum Gene Ther*. 2014;25(5):461–474.
- Passini MA, Wolfe JH. Widespread gene delivery and structure-specific patterns of expression in the brain after intraventricular injections of neonatal mice with an adeno-associated virus vector. *J Virol*. 2001;75(24):12382–12392.
- Xhima K, Nabbouh F, Hynynen K, Aubert I, Tandon A. Noninvasive delivery of an alpha-synuclein gene silencing vector with magnetic resonance-guided focused ultrasound. *Mov Disord*. 2018;33(10):1567–1579.
- Newell KL, Boyer P, Gomez-Tortosa E, et al. Alpha-synuclein immunoreactivity is present in axonal swellings in neuroaxonal dystrophy and acute traumatic brain injury. *J Neuropathol Exp Neurol*. 1999;58(12):1263–1268.
- Sacino AN, Brooks M, McKinney AB, et al. Brain injection of alpha-synuclein induces multiple proteinopathies, gliosis, and a neuronal injury marker. *J Neurosci*. 2014;34(37):12368–12378.
- Delic V, Beck KD, Pang KCH, Citron BA. Biological links between traumatic brain injury and Parkinson's disease. *Acta Neuropathol Commun*. 2020;8(1):45.
- Hasan S, Mielke MM, Turcano P, Ahlskog JE, Bower JH, Savica R. Traumatic brain injury preceding clinically diagnosed alpha-synucleinopathies: A case-control study. *Neurology*. 2020;94(8):e764–e773.
- Zhang SJ, Ye J, Miao C, et al. Optogenetic dissection of entorhinal-hippocampal functional connectivity. *Science*. 2013;340(6128): 1232627.
- Aschauer DF, Kreuz S, Rumpel S. Analysis of transduction efficiency, tropism and axonal transport of AAV serotypes 1, 2, 5, 6, 8 and 9 in the mouse brain. *PLoS One*. 2013;8(9):e76310.

32. Zingg B, Chou XL, Zhang ZG, et al. AAV-mediated anterograde transsynaptic tagging: Mapping corticocollicular input-defined neural pathways for defense behaviors. *Neuron*. 2017;93(1):33–47.
33. Kim ST, Son HJ, Choi JH, Ji IJ, Hwang O. Vertical grid test and modified horizontal grid test are sensitive methods for evaluating motor dysfunctions in the MPTP mouse model of Parkinson's disease. *Brain Res*. 2010;1306:176–183.
34. Kuusisto E, Salminen A, Alafuzoff I. Ubiquitin-binding protein p62 is present in neuronal and glial inclusions in human tauopathies and synucleinopathies. *Neuroreport*. 2001;12(10):2085–2090.
35. Zatloukal K, Stumpfner C, Fuchsichler A, et al. p62 Is a common component of cytoplasmic inclusions in protein aggregation diseases. *Am J Pathol*. 2002;160(1):255–263.
36. Kuusisto E, Parkkinen L, Alafuzoff I. Morphogenesis of Lewy bodies: Dissimilar incorporation of alpha-synuclein, ubiquitin, and p62. *J Neuropathol Exp Neurol*. 2003;62(12):1241–1253.
37. Cuervo AM, Stefanis L, Fredenburg R, Lansbury PT, Sulzer D. Impaired degradation of mutant alpha-synuclein by chaperone-mediated autophagy. *Science*. 2004;305(5688):1292–1295.
38. Winslow AR, Chen CW, Corrochano S, et al. alpha-Synuclein impairs macroautophagy: Implications for Parkinson's disease. *J Cell Biol*. 2010;190(6):1023–1037.
39. Gorbatyuk OS, Li S, Nash K, et al. In vivo RNAi-mediated alpha-synuclein silencing induces nigrostriatal degeneration. *Mol Ther*. 2010;18(8):1450–1457.
40. Collier TJ, Redmond DE Jr., Steece-Collier K, Lipton JW, Manfredsson FP. Is alpha-synuclein loss-of-function a contributor to parkinsonian pathology? Evidence from non-human primates. *Front Neurosci*. 2016;10:12.
41. Benskey MJ, Sellnow RC, Sandoval IM, Sortwell CE, Lipton JW, Manfredsson FP. Silencing alpha synuclein in mature nigral neurons results in rapid neuroinflammation and subsequent toxicity. *Front Mol Neurosci*. 2018;11:36.
42. Gelders G, Baekelandt V, Van der Perren A. Linking neuroinflammation and neurodegeneration in Parkinson's disease. *J Immunol Res*. 2018;2018:4784268.
43. Asher DM, Belay E, Bigio E, et al. Risk of transmissibility from neurodegenerative disease-associated proteins: Experimental knowns and unknowns. *J Neuropathol Exp Neurol*. 2020;79(11):1141–1146.
44. Steiner JA, Quansah E, Brundin P. The concept of alpha-synuclein as a prion-like protein: Ten years after. *Cell Tissue Res*. 2018;373(1):161–173.
45. Rodriguez L, Marano MM, Tandon A. Import and export of misfolded alpha-synuclein. *Front Neurosci*. 2018;12:344.
46. Rusten TE, Stenmark H. p62, an autophagy hero or culprit? *Nat Cell Biol*. 2010;12(3):207–209.
47. Crews L, Spencer B, Desplats P, et al. Selective molecular alterations in the autophagy pathway in patients with Lewy body disease and in models of alpha-synucleinopathy. *PLoS One*. 2010;5(2):e9313.
48. Lindersson E, Beedholm R, Hojrup P, et al. Proteasomal inhibition by alpha-synuclein filaments and oligomers. *J Biol Chem*. 2004;279(13):12924–12934.
49. Emmanouilidou E, Stefanis L, Vekrellis K. Cell-produced alpha-synuclein oligomers are targeted to, and impair, the 26S proteasome. *Neurobiol Aging*. 2010;31(6):953–968.
50. Decressac M, Mattsson B, Weikop P, Lundblad M, Jakobsson J, Björklund A. TFEB-mediated autophagy rescues midbrain dopamine neurons from alpha-synuclein toxicity. *Proc Natl Acad Sci U S A*. 2013;110(19):E1817–E1826.
51. Lee HJ, Cho ED, Lee KW, Kim JH, Cho SG, Lee SJ. Autophagic failure promotes the exocytosis and intercellular transfer of alpha-synuclein. *Exp Mol Med*. 2013;45:e22.
52. Wildburger NC, Hartke AS, Schidlitzki A, Richter F. Current evidence for a bidirectional loop between the lysosome and alpha-synuclein proteoforms. *Front Cell Dev Biol*. 2020;8:598446.
53. Zheng Y-Q, Zhang Y, Yau Y, et al. Local vulnerability and global connectivity jointly shape neurodegenerative disease propagation. *PLoS Biol*. 2019;17(11):e3000495.
54. Gribaudo S, Tixador P, Bousset L, et al. Propagation of alpha-synuclein strains within human reconstructed neuronal network. *Stem Cell Rep*. 2019;12(2):230–244.
55. Mezas C, Rey N, Brundin P, Raj A. Neural connectivity predicts spreading of alpha-synuclein pathology in fibril-injected mouse models: Involvement of retrograde and anterograde axonal propagation. *Neurobiol Dis*. 2020;134:104623.
56. Luk KC, Kehm VM, Zhang B, O'Brien P, Trojanowski JQ, Lee VM. Intracerebral inoculation of pathological alpha-synuclein initiates a rapidly progressive neurodegenerative alpha-synucleinopathy in mice. *J Exp Med*. 2012;209(5):975–986.
57. Kim YC, Miller A, Lins LC, et al. RNA interference of human alpha-synuclein in mouse. *Front Neurol*. 2017;8:13.
58. Alarcon-Aris D, Recasens A, Galofre M, et al. Selective alpha-synuclein knockdown in monoamine neurons by intranasal oligonucleotide delivery: Potential therapy for Parkinson's disease. *Mol Ther*. 2018;26(2):550–567.
59. Zharikov A, Bai Q, De Miranda BR, Van Laar A, Greenamyre JT, Burton EA. Long-term RNAi knockdown of alpha-synuclein in the adult rat substantia nigra without neurodegeneration. *Neurobiol Dis*. 2019;125:146–153.
60. Izco M, Blesa J, Schleeff M, et al. Systemic exosomal delivery of shRNA minicircles prevents parkinsonian pathology. *Mol Ther*. 2019;27(12):2111–2122.
61. Alarcon-Aris D, Pavia-Collado R, Miquel-Rio L, et al. Anti-alpha-synuclein ASO delivered to monoamine neurons prevents alpha-synuclein accumulation in a Parkinson's disease-like mouse model and in monkeys. *EBioMedicine*. 2020;59:102944.
62. Cole TA, Zhao H, Collier TJ, et al. alpha-Synuclein antisense oligonucleotides as a disease-modifying therapy for Parkinson's disease. *JCI Insight*. 2021;6(5):e135633.
63. Weber Boutros S, Raber J, Unni VK. Effects of alpha-synuclein targeted antisense oligonucleotides on Lewy body-like pathology and behavioral disturbances induced by injections of pre-formed fibrils in the mouse motor cortex. *J Parkinsons Dis*. 2021;11(3):1091–1115.
64. Pavia-Collado R, Coppola-Segovia V, Miquel-Rio L, et al. Intracerebral administration of a ligand-ASO conjugate selectively reduces alpha-synuclein accumulation in monoamine neurons of double mutant human A30PA53Talpha-synuclein transgenic mice. *Int J Mol Sci*. 2021;22(6):2939.
65. Yang J, Luo S, Zhang J, et al. Exosome-mediated delivery of antisense oligonucleotides targeting alpha-synuclein ameliorates the pathology in a mouse model of Parkinson's disease. *Neurobiol Dis*. 2021;148:105218.
66. Bruck D, Wenning GK, Stefanova N, Fellner L. Glia and alpha-synuclein in neurodegeneration: A complex interaction. *Neurobiol Dis*. 2016;85:262–274.
67. Refolo V, Stefanova N. Neuroinflammation and glial phenotypic changes in alpha-synucleinopathies. *Front Cell Neurosci*. 2019;13:263.
68. Shavali S, Combs CK, Ebadi M. Reactive macrophages increase oxidative stress and alpha-synuclein nitration during death of dopaminergic neuronal cells in co-culture: Relevance to Parkinson's disease. *Neurochem Res*. 2006;31(1):85–94.
69. Gao HM, Kotzbauer PT, Uryu K, Leight S, Trojanowski JQ, Lee VM. Neuroinflammation and oxidation/nitration of alpha-synuclein linked to dopaminergic neurodegeneration. *J Neurosci*. 2008;28(30):7687–7698.
70. Guo M, Wang J, Zhao Y, et al. Microglial exosomes facilitate alpha-synuclein transmission in Parkinson's disease. *Brain*. 2020;143(5):1476–1497.
71. Chatterjee D, Kordower JH. Immunotherapy in Parkinson's disease: Current status and future directions. *Neurobiol Dis*. 2019;132:104587.

72. Shin J, Kim HJ, Jeon B. Immunotherapy targeting neurodegenerative proteinopathies: Alpha-synucleinopathies and tauopathies. *J Mov Disord.* 2020;13(1):11–19.
73. Volc D, Poewe W, Kutzelnigg A, et al. Safety and immunogenicity of the alpha-synuclein active immunotherapeutic PD01A in patients with Parkinson's disease: A randomised, single-blinded, phase 1 trial. *Lancet Neurol.* 2020;19(7):591–600.
74. Meissner WG, Traon AP, Foubert-Samier A, et al.; AFF009 Study Investigators. A phase 1 randomized trial of specific active alpha-synuclein immunotherapies PD01A and PD03A in multiple system atrophy. *Mov Disord.* 2020;35(11):1957–1965.
75. Jankovic J, Goodman I, Safirstein B, et al. Safety and tolerability of multiple ascending doses of PRX002/RG7935, an anti-alpha-synuclein monoclonal antibody, in patients with Parkinson disease: A randomized clinical trial. *JAMA Neurol.* 1 2018;75(10):1206–1214.
76. Kuchimanchi M, Monine M, Kandadi Muralidharan K, Woodward C, Penner N. Phase II dose selection for alpha synuclein-targeting antibody cinpanemab (BIIB054) based on target protein binding levels in the brain. *CPT Pharmacometrics Syst Pharmacol.* 2020;9(9):515–522.
77. Mittal S, Bjernevik K, Im DS, et al. beta2-Adrenoreceptor is a regulator of the alpha-synuclein gene driving risk of Parkinson's disease. *Science.* 1 2017;357(6354):891–898.
78. Sardi SP, Viel C, Clarke J, et al. Glucosylceramide synthase inhibition alleviates aberrations in synucleinopathy models. *Proc Natl Acad Sci U S A.* 2017;114(10):2699–2704.
79. Savitt D, Jankovic J. Targeting alpha-synuclein in Parkinson's disease: Progress towards the development of disease-modifying therapeutics. *Drugs.* 2019;79(8):797–810.
80. Mullin S, Smith L, Lee K, et al. Ambroxol for the treatment of patients with Parkinson disease with and without glucocerebrosidase gene mutations: A nonrandomized, noncontrolled trial. *JAMA Neurol.* 2020;77(4):427–434.
81. Han TU, Sam R, Sidransky E. Small molecule chaperones for the treatment of Gaucher disease and GBA1-associated Parkinson disease. *Front Cell Dev Biol.* 2020;8:271.
82. Uehara T, Choong CJ, Nakamori M, et al. Amido-bridged nucleic acid (AmNA)-modified antisense oligonucleotides targeting alpha-synuclein as a novel therapy for Parkinson's disease. *Sci Rep.* 2019;9(1):7567.
83. Hitti FL, Yang AI, Gonzalez-Alegre P, Baltuch GH. Human gene therapy approaches for the treatment of Parkinson's disease: An overview of current and completed clinical trials. *Parkinsonism Relat Disord.* 2019;66:16–24.
84. Nuber S, Petrasch-Parwez E, Winner B, et al. Neurodegeneration and motor dysfunction in a conditional model of Parkinson's disease. *J Neurosci.* 2008;28(10):2471–2484.
85. Cooper JM, Wiklander PB, Nordin JZ, et al. Systemic exosomal siRNA delivery reduced alpha-synuclein aggregates in brains of transgenic mice. *Mov Disord.* 2014;29(12):1476–1485.
86. Miller DB, O'Callaghan JP. Biomarkers of Parkinson's disease: Present and future. *Metabolism.* 2015;64(3 Suppl 1):S40–S46.
87. Heinzel S, Berg D, Gasser T, et al.; MDS Task Force on the Definition of Parkinson's Disease. Update of the MDS research criteria for prodromal Parkinson's disease. *Mov Disord.* 2019;34(10):1464–1470.
88. Pedersen CC, Lange J, Førlund MGG, Macleod AD, Alves G, Maple-Grødem J. A systematic review of associations between common SNCA variants and clinical heterogeneity in Parkinson's disease. *NPJ Parkinsons Dis.* 2021;7(1):54.
89. Farrer M, Kachergus J, Forno L, et al. Comparison of kindreds with parkinsonism and alpha-synuclein genomic multiplications. *Ann Neurol.* 2004;55(2):174–179.
90. Kordower JH, Chu Y, Hauser RA, Freeman TB, Olanow CW. Lewy body-like pathology in long-term embryonic nigral transplants in Parkinson's disease. *Nat Med.* 2008;14(5):504–506.
91. Li JY, Englund E, Holton JL, et al. Lewy bodies in grafted neurons in subjects with Parkinson's disease suggest host-to-graft disease propagation. *Nat Med.* 2008;14(5):501–503.
92. Kahle PJ, Neumann M, Ozmen L, et al. Hyperphosphorylation and insolubility of {alpha}-synuclein in transgenic mouse oligodendrocytes. *EMBO Rep.* 2002;3(6):583–588.
93. Shults CW, Rockenstein E, Crews L, et al. Neurological and neurodegenerative alterations in a transgenic mouse model expressing human alpha-synuclein under oligodendrocyte promoter: Implications for multiple system atrophy. *J Neurosci.* 2005;25(46):10689–10699.
94. Yazawa I, Giasson BI, Sasaki R, et al. Mouse model of multiple system atrophy alpha-synuclein expression in oligodendrocytes causes glial and neuronal degeneration. *Neuron.* 2005;45(6):847–859.
95. Torregrosa T, Lehman S, Hana S, et al. Use of CRISPR/Cas9-mediated disruption of CNS cell type genes to profile transduction of AAV by neonatal intracerebroventricular delivery in mice. *Gene Ther.* 2021;28(7-8):456–468.
96. Del Tredici K, Rub U, de Vos RA, Bohl JR, Braak H. Where does Parkinson disease pathology begin in the brain? *J Neuropathol Exp Neurol.* 2002;61(5):413–426.
97. Braak H, Tredici KD, Rub U, de Vos RA, Jansen Steur EN, Braak E. Staging of brain pathology related to sporadic Parkinson's disease. *Neurobiol Aging.* 2003;24(2):197–211.
98. Braak H, Del Tredici K. Nervous system pathology in sporadic Parkinson disease. *Neurology.* 2008;70(20):1916–1925.
99. Postuma RB, Berg D. Advances in markers of prodromal Parkinson disease. *Nat Rev Neurol.* 2016;12(11):622–634.
100. Lipsman N, Meng Y, Bethune AJ, et al. Blood-brain barrier opening in Alzheimer's disease using MR-guided focused ultrasound. *Nat Commun.* 2018;9(1):2336.
101. Gasca-Salas C, Fernandez-Rodriguez B, Pineda-Pardo JA, et al. Blood-brain barrier opening with focused ultrasound in Parkinson's disease dementia. *Nat Commun.* 2021;12(1):779-